

<sup>1</sup> Increasing prevalence of plant-fungal symbiosis across two  
<sup>2</sup> centuries of environmental change

<sup>3</sup> Joshua C. Fowler<sup>1,2\*</sup>

Jacob Moutouama<sup>1,3</sup>

Tom E. X. Miller<sup>1</sup>

<sup>4</sup> 1. Rice University, Department of BioSciences, Houston, Texas 77006; 2. University of Miami,  
<sup>5</sup> Department of Biology, Miami, Florida; 3. Department of Botany, University of British Columbia,  
<sup>6</sup> 6270 University Blvd, Vancouver, BC V6T 1Z4

<sup>7</sup> \* Corresponding author; e-mail: jcf221@miami.edu.

<sup>8</sup> *Manuscript elements:* Figure 1 - Figure 6, Appendix A (including Figure A1 - Figure A15, Table  
<sup>9</sup> A1, and Supporting Methods).

<sup>10</sup> *Keywords:* climate change, *Epichloë*, herbarium, INLA, museum specimen, plant-microbe sym-  
<sup>11</sup> biosis, Poaceae, spatially-varying coefficients model

<sup>12</sup> *Manuscript type:* Research Article.

## Abstract

Species' distributions and abundances are shifting in response to ongoing global climate change. Mutualistic microbial symbionts can provide hosts with protection from environmental stress that may promote resilience under environmental change, however this change may also disrupt species interactions and lead to declines in hosts and/or symbionts. Symbionts preserved within natural history specimens offer a unique opportunity to quantify changes in microbial symbiosis across broad temporal and spatial scales. We asked how the prevalence of seed-transmitted fungal symbionts of grasses (*Epichloë* endophytes) has changed over time in response to climate change, and how these changes vary across host species' distributions. Specifically, we examined 2,346 herbarium specimens of three grass host species (*Agrostis hyemalis*, *Agrostis perennans*, *Elymus virginicus*) collected over the past two centuries (1824 – 2019) for the presence or absence of *Epichloë* symbiosis. Analysis of an approximate Bayesian spatially-varying coefficients model revealed that endophytes increased in prevalence over the last two centuries from ca. 25% to ca. 75% prevalence, on average, across three host species. Changes in seasonal climate drivers were associated with increasing endophyte prevalence. Notably, increasing precipitation during the peak growing season for *Agrostis* species and decreasing precipitation for *E. virginicus* were associated with increasing endophyte prevalence. Changes in the variability of precipitation and temperature during off-peak seasons were also important predictors of increasing endophyte prevalence. Our model performed favorably in an out-of-sample predictive test with contemporary survey data from across 63 populations, a rare extra step in collections-based research. However, there was greater local-scale variability in endophyte prevalence in contemporary data compared to model predictions, suggesting new directions that could improve predictive accuracy. Our results provide novel evidence for a cryptic biological response to climate change that may contribute to the resilience of host-microbe symbiosis through fitness benefits to symbiotic hosts.

## Introduction

38 Understanding how biotic interactions are altered by global change is a major goal of basic and  
39 applied ecological research (Blois et al., 2013; Gilman et al., 2010). Documented responses to envi-  
40 ronmental change, such as shifts in species' distributions (Aitken et al., 2008) and phenology (Piao  
41 et al., 2019), are typically blind to concurrent changes in associated biotic interactions. Empirically  
42 evaluating these biotic changes – whether interacting species shift in tandem with their partners  
43 or not (HilleRisLambers et al., 2013) – is crucial to predicting the reorganization of Earth's biodi-  
44 versity under global change. Such evaluations have been limited because few datasets on species  
45 interactions extend over sufficiently long time scales of contemporary climate change (Poisot et al.,  
46 2021).

47 Natural history specimens, which were originally collected to document and preserve taxonomic  
48 diversity, present a unique opportunity to explore long-term changes in biodiversity and ecological  
49 interactions across broad spatial and temporal scales (Davis, 2023; Meineke et al., 2018). Natural  
50 history collections, built and maintained by the efforts of thousands of scientists, are invaluable  
51 time machines, primarily comprised of physical specimens of organisms along with information  
52 about the time and place of their collection. These specimens often preserve physical legacies  
53 of ecological processes and species' interactions from dynamically changing environments across  
54 time and space (Lendemer et al., 2020). For example, previous researchers have examined the  
55 flowers, pollen grains, and leaves of specimens within plant collections (herbaria) to document shifts  
56 in reproductive phenology (Berg et al., 2019; Park et al., 2019; Willis et al., 2017), pollination  
57 (Duan et al., 2019; Pauw and Hawkins, 2011), and herbivory (Meineke et al., 2019) related to  
58 anthropogenic climate change. Herbarium specimens have also been used to identify the origins  
59 and population genomics of plant diseases such as *Phytophthora*, the Irish potato famine pathogen  
60 (Ristaino et al., 2001; Ristaino, 2002; Yoshida et al., 2013), and have been proposed as vehicles  
61 to track other emerging plant pathogens (Bradshaw et al., 2021; Ristaino, 2020). However, few  
62 previous studies have leveraged biological collections to examine climate change-related shifts in a

63 particularly common type of interaction: mutualistic microbial symbiosis.

64 Microbial symbionts are common to all macroscopic organisms and can have important effects  
65 on their hosts' survival, growth and reproduction (McFall-Ngai et al., 2013; Rodriguez et al., 2009).  
66 Many microbial symbionts act as mutualists, engaging in reciprocally beneficial interactions with  
67 their hosts in ways that can ameliorate environmental stress. For example, bacterial symbionts of  
68 insects, such as *Wolbachia*, can improve their hosts' thermal tolerance (Reno et al., 2019; Truitt  
69 et al., 2019), and arbuscular mycorrhizal fungi, documented in 70-90% of families of land plants  
70 (Parniske, 2008), allow their hosts to persist through drought conditions by improving water and  
71 nutrient uptake (Cheng et al., 2021). On the other hand, changes in the mean and variance of  
72 environmental conditions may disrupt microbial mutualisms by changing the costs and benefits  
73 of the interaction for each partner in ways that can cause the interaction to deteriorate (Aslan  
74 et al., 2013; Fowler et al., 2024). Coral bleaching (the loss of symbiotic algae) due to temperature  
75 stress (Sully et al., 2019) is perhaps the best known example, but this phenomenon is not unique  
76 to corals. Lichens exposed to elevated temperatures experienced loss of photosynthetic function  
77 along with changes in the composition of their algal symbiont community (Meyer et al., 2022).  
78 How commonly and under what conditions microbial mutualisms deteriorate or strengthen under  
79 climate change remain unanswered questions (Frederickson, 2017). Previous work suggests that  
80 these alternative responses may depend on the intimacy and specialization of the interaction as well  
81 as the physiological tolerances of the mutualist partners (Rafferty et al., 2015; Toby Kiers et al.,  
82 2010; Warren and Bradford, 2014).

83 Understanding how microbial symbioses are affected by climate change is additionally compli-  
84 cated by spatial heterogeneity in the direction and magnitude of environmental change (IPCC, 2021).  
85 Beneficial symbionts are likely able to shield their hosts from environmental stress in locations that  
86 experience a small degree of change, but symbionts in locations that experience changes of large  
87 magnitude may be pushed beyond their physiological limits (Webster et al., 2008). Additionally,  
88 symbionts are often unevenly distributed across their host's distribution. Facultative symbionts  
89 may be absent from portions of the host range (Afkhami et al., 2014), and hosts may engage with

90 a diversity of partners (different symbiont species or locally-adapted strains) across environments  
91 (Fowler et al., 2023; Fraude et al., 2008; Rolshausen et al., 2018). Identifying broader spatial trends  
92 in symbiont prevalence is therefore an important step in developing predictions for where to expect  
93 changes in the symbiosis in future climates.

94 *Epichloë* fungal endophytes are specialized symbionts of cool-season grasses, documented in  
95 ~ 30% of cool-season grass species (Leuchtmann, 1992). They are predominantly transmitted ver-  
96 tically from maternal plants to offspring through seeds. Vertical transmission creates a feedback  
97 between the fitness of host and symbiont (Douglas, 1998; Fine, 1975; Rudgers et al., 2009). Over  
98 time, endophytes that act as mutualists should rise in prevalence within a host population, partic-  
99 ularly under environmental conditions that elicit protective benefits (Donald et al., 2021). *Epichloë*  
100 are known to improve their hosts' drought tolerance (Decunta et al., 2021) and protect their hosts  
101 against herbivores (Crawford et al., 2010) and pathogens (Xia et al., 2018) likely through the pro-  
102 duction of a diverse suite of alkaloids and other secondary metabolites. The fitness feedback induced  
103 by vertical transmission leads to the prediction that endophyte prevalence should be high in pop-  
104 ulations where these fitness benefits are most important. Previous survey studies of contemporary  
105 populations have documented large-scale spatial patterns in endophyte prevalence structured by  
106 environmental gradients (Afkhami, 2012; Bazely et al., 2007; Granath et al., 2007; Sneck et al.,  
107 2017). We predicted that endophyte prevalence should track temporal changes in environmental  
108 drivers (i.e. drought) that elicit strong fitness benefits.

109 Early research on *Epichloë* used herbarium specimens to describe the broad taxonomic diversity  
110 of grass host species that harbor these symbionts (White and Cole, 1985), establishing that endo-  
111 phyte symbiosis could be identified in plant tissue from as early as 1851. However, no subsequent  
112 studies, to our knowledge, have used the vast resources of biological collections to quantitatively  
113 assess spatio-temporal trends in endophyte prevalence and their environmental correlates. Grasses  
114 are commonly collected and identified based on the presence of their reproductive structures, mean-  
115 ing that preserved specimens typically contain seeds, conveniently preserving the seed-transmitted  
116 fungi along with their host plants on herbarium sheets. This creates the opportunity to leverage

117 the unique spatio-temporal sampling of herbarium collections to examine the response of this sym-  
118 biosis to historical climate change. However, the predictive ability derived from historical analyses  
119 is rarely tested against contemporary data (Lee et al., 2024). Critically evaluating whether insights  
120 from historical reconstruction are predictive of variation across contemporary populations is a cru-  
121 cial step for the field to move from reading signatures of the past to forecasting ecological dynamics  
122 into the future.

123 In this study, we assessed the long-term responses of *Epichloë* endophyte symbiosis to climate  
124 change through the use of herbarium specimens of three North American host grass species (*Agrostis*  
125 *hyemalis*, *Agrostis perennans*, and *Elymus virginicus*). We first addressed questions describing  
126 spatial and temporal trends in endophyte prevalence: (i) How has endophyte prevalence changed  
127 over the past two centuries? and (ii) How spatially variable are temporal trends in endophyte  
128 prevalence across eastern North America? We then addressed how climate change may be driving  
129 trends in endophyte prevalence by asking: (iii) What is the relationship between temporal trends  
130 in endophyte prevalence and associated changes in climate drivers? We predicted that overall  
131 endophyte prevalence would increase over time in tandem with climate change, and that localized  
132 hotspots of endophyte change would correspond spatially to hotspots of climate warming and drying.  
133 Finally, we evaluated (iv) how our model, built on data from historic specimens, performed in an out-  
134 of-sample test using data on endophyte prevalence from contemporary surveys of host populations.  
135 To answer these questions we examined a total of 2,346 historic specimens collected across eastern  
136 North America between 1824 and 2019, and evaluated model performance against contemporary  
137 surveys comprising 1,442 individuals from 63 populations surveyed between 2013 and 2020.

138 **Methods**

139 *Focal species*

140 Our surveys focused on three native North American grasses: *Agrostis hyemalis*, *Agrostis perennans*,  
141 and *Elymus virginicus* that host *Epichloë* symbionts. These cool-season grass species have broad

<sup>142</sup> distributions covering much the eastern United States (Fig. 1) and are commonly represented in  
<sup>143</sup> natural history collections. Cool-season grasses grow during the cooler temperatures of spring and  
<sup>144</sup> autumn due to their reliance on  $C_3$  photosynthesis. *A. hyemalis* is a small short-lived perennial  
<sup>145</sup> species that germinates in autumn to late winter winter and typically flowers between March and  
<sup>146</sup> July (most common collection month: May). *A. perennans* is of similar stature but is longer lived  
<sup>147</sup> than *Agrostis hyemalis* and flowers in late summer and early autumn (most common collection  
<sup>148</sup> month: September). *A. perennans* is more sparsely distributed, tending to be found in shadier and  
<sup>149</sup> moister habitats, while *A. hyemalis* is commonly found in open and recently disturbed habitats.  
<sup>150</sup> Both *Agrostis* species are recorded from throughout the Eastern US, but *A. perennans* has a slightly  
<sup>151</sup> more northern distribution, whereas *A. hyemalis* is found rarely as far north as Canada and is listed  
<sup>152</sup> as a rare plant in Minnesota. *E. virginicus* is a larger and longer-lived species that is more broadly  
<sup>153</sup> distributed than the *Agrostis* species. It begins flowering as early as March or April but continues  
<sup>154</sup> throughout the summer (most common collection month: July).

<sup>155</sup> Both *Agrostis* species host *Epichloë amarillans* (Craven et al., 2001; Leuchtmann et al., 2014),  
<sup>156</sup> and *Elymus virginicus* typically hosts *Epichloë elymi* (Clay and Schardl, 2002). The fungal sym-  
<sup>157</sup> bionts primarily reproduce asexually and are passed from maternal plant to offspring by vertical  
<sup>158</sup> transmission through seeds. Some host species have been shown to partner with multiple symbiont  
<sup>159</sup> species or strains, and in some cases multiple symbiont lineages can co-exist within a host popu-  
<sup>160</sup> lation (Mc Cargo et al., 2014). However, surveys have typically found limited *Epichloë* genotypic  
<sup>161</sup> diversity within host populations (Treindl et al., 2023). Across host populations, concentrations  
<sup>162</sup> of biologically-active alkaloids and the genes associated with their production vary substantially  
<sup>163</sup> (Schardl et al., 2012). In this analysis, we focus on the presence/absence of *Epichloë* symbionts,  
<sup>164</sup> and we discuss potential implications of symbiont genotypic diversity in the Discussion.

<sup>165</sup> *Herbarium surveys*

<sup>166</sup> We visited nine herbaria between 2019 and 2022 (see Table A1 for a summary of specimens included  
<sup>167</sup> from each collection). With permission from herbarium staff, we acquired seed samples from 1135

168 *A. hyemalis* specimens collected between 1824 and 2019, 357 *A. perennans* specimens collected  
169 between 1863 and 2017, and 854 *E. virginicus* specimens collected between 1839 and 2019 (Fig. 1,  
170 Fig. 2A, Fig. A1). We chose our focal species in part because they are commonly represented in  
171 herbarium collections and produce many seeds, meaning that small samples would not diminish the  
172 value of specimens for future studies. We collected 5-10 seeds per specimen after examining the  
173 herbarium sheet under a dissecting microscope to ensure that we collected mature seeds, not florets  
174 or unfilled seeds, fit for our purpose of identifying fungal endophytes with microscopy. We excluded  
175 specimens for which information about the collection location and date were unavailable.

176 Each specimen was assigned geographic coordinates based on collection information recorded on  
177 the herbarium sheet using the geocoding functionality of the *ggmap* R package (Kahle and Wickham,  
178 2019). Many specimens had digitized collection information readily available, but for those that  
179 did not, we transcribed information printed on the herbarium sheet. The identity of each specimen  
180 collector was gathered as part of the sample's metadata. Collections were geo-referenced to the  
181 nearest county centroid, or nearest municipality when that information was available. For fifteen  
182 of the oldest specimens, only information at the state level was available, and so we used the state  
183 centroid. The median pairwise distance between georeferenced coordinate points was 841 km. The  
184 median longitudinal width of the bounding boxes generated to geocode municipality, county, or  
185 state centroids was 44.7 km. Among those specimens geo-referenced at the state level, the largest  
186 bounding box, spanning the state of Texas, was 1233 km wide. The smallest bounding boxes were  
187 less than 1 km across for small municipalities (while this suggests high precision, we note that some  
188 specimens were collected in natural habitat nearby to small municipalities not encompassed by these  
189 bounding boxes).

190 Our visits focused on herbaria with historic strengths in grass collections (e.g. Texas A&M,  
191 Missouri Botanic Garden) and other herbaria in the Southern Great Plains region of the United  
192 States. While these nine herbaria garnered specimens that span the focal species' ranges, our dataset  
193 unevenly samples across the study region (Fig. 1). Texas, Oklahoma, Louisiana, and Missouri are  
194 the most represented states. Uneven sampling was most pronounced for *A. perennans*, which has

195 much of its range in the northeastern US. We explore the potential influence of spatial bias in  
196 sampling on our results through a simulation analysis (Appendix A - Supporting Methods).

197 After collecting seed samples, we quantified the presence or absence of *Epichloë* fungal hyphae  
198 in each specimen using microscopy. We first softened seeds with a 10% NaOH solution, then stained  
199 the seeds with aniline blue-lactic acid stain and squashed them under a microscope cover slip. We  
200 examined the squashed seeds for the presence of fungal hyphae at 200-400X magnification (Bacon  
201 and White, 2018). On average we scored 4.7 intact seeds per specimen of *A. hyemalis*, 4.2 seeds  
202 per specimen of *A. perennans*, and 3.8 seeds per specimen of *E. virginicus*; we scored 10,342 seeds  
203 in total. Due to imperfect vertical transmission, the production of symbiont-free offspring from  
204 symbiotic hosts (Afkhami and Rudgers, 2008), it is possible that symbiotic host-plants produce a  
205 mixture of symbiotic and non-symbiotic seeds. We therefore designated a specimen as endophyte-  
206 symbiotic if *Epichloë* hyphae were observed in one or more of its seeds, or non-symbiotic if *Epichloë*  
207 hyphae were observed in none of its seeds. To capture uncertainty in the endophyte identification  
208 process, we recorded both a "liberal" and a "conservative" endophyte score for each plant specimen.  
209 When we confidently identified endophytes within a specimen's seeds, we assigned matching liberal  
210 and conservative scores. When we identified potential endophytes with unusual morphology, low  
211 uptake of stain, or a small amount of fungal hyphae across the scored seeds, we recorded a positive  
212 identification for the liberal score and a negative identification for the conservative score. We  
213 recorded the identity of each scorer as part of the data collection process. 89% of scored plants  
214 had matching liberal and conservative scores, reflecting high confidence in endophyte status. The  
215 following analyses used the liberal status, however repeating all analyses with the conservative status  
216 yielded qualitatively similar results (Fig. A8).

217 *Modeling spatial and temporal changes in endophyte prevalence*

218 We assessed spatial and temporal changes in endophyte prevalence across each host distribution,  
219 quantifying the "global" temporal trends averaged across space, and then examining spatial hetero-  
220 geneity in the direction and magnitude of endophyte change (hotspots and coldspots) across the spa-

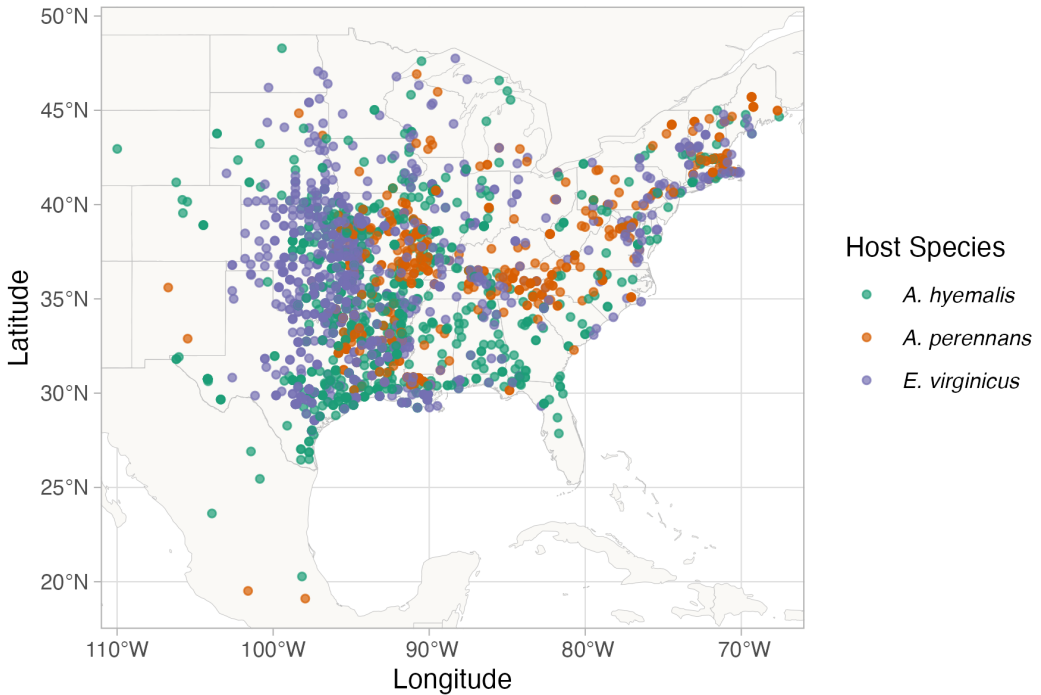


Figure 1: Collection locations of herbarium specimens sampled for *Epichloë* endophytes.

Specimens span eastern North America from nine herbaria, and are colored by host species (*A. hyemalis*: green, *A. perennans*: orange, *E. virginicus*: purple). Map lines delineate study areas and do not necessarily depict accepted national boundaries.

trial extent of each host's distribution. To account for the spatial non-independence of geo-referenced occurrences, we used an approximate Bayesian method, Integrated Nested Laplace Approximation (INLA), to construct spatio-temporal models of endophyte prevalence. INLA provides a computationally efficient method of ascertaining parameter posterior distributions for certain models that can be formulated as latent Gaussian Models (Rue et al., 2009). Many common statistical models, including structured and unstructured mixed-effects models, can be represented as latent Gaussian Models. We incorporated spatial heterogeneity into this analysis using spatially-structured intercept and slope parameters implemented as stochastic partial differential equations (SPDE) to approximate a continuous spatial Gaussian process. This SPDE approach is a flexible method of smoothing across space while explicitly accounting for spatial dependence between data-points (Bakka et al.,

231 2018; Lindgren et al., 2011). Fitting models with structured spatial effects is possible with MCMC  
232 sampling but can require long computation times, making INLA an effective alternative. This ap-  
233 proach has been used to model spatial patterns in flowering phenology (Willems et al., 2022), the  
234 abundance of birds (Meehan et al., 2019) and butterflies (Crossley et al., 2022), the distribution of  
235 temperate trees (Engel et al., 2022) as well as the population dynamics of endangered amphibians  
236 (Knapp et al., 2016) and other ecological processes (Beguin et al., 2012).

237 We estimated global and spatially-varying trends in endophyte prevalence using a joint-likelihood  
238 model. For each host species  $h$ , endophyte presence/absence of the  $i^{th}$  specimen ( $P_{h,i}$ ) was modeled  
239 as a Bernoulli response variable with expected probability of endophyte occurrence  $\hat{P}_{h,i}$ . We modeled  
240  $\hat{P}_{h,i}$  as a linear function of collection year, with intercept  $A_h$  and slope  $T_h$  defining the global  
241 temporal trend in endophyte prevalence specific to each host species as well as with spatially-  
242 varying intercepts  $\alpha_{h,l_i}$  and slopes  $\tau_{h,l_i}$  associated with location ( $l_i$ , the unique latitude-longitude  
243 combination of the  $i^{th}$  observation). The joint-model structure allowed us to “borrow information”  
244 across species in the estimation of shared variance terms for the spatially-dependent random effect  
245  $\delta_{l_i}$ , intended to account for residual spatial variation, and  $\chi_{c_i}$  and  $\omega_{s_i}$ , the i.i.d.-random effects  
246 indexed for each collector identity ( $c_i$ ) and scorer identity ( $s_i$ ) of the  $i^{th}$  specimen.

$$\text{logit}(\hat{P}_{h,i}) = A_h + T_h * \text{year}_i + \alpha_{h,l_i} + \tau_{h,l_i} * \text{year}_i + \delta_{l_i} + \chi_{c_i} + \omega_{s_i} \quad (1)$$

247 By including random effects for collectors and scorers, we accounted for “nuisance” variance that  
248 may bias predictions for changes in endophyte prevalence. Previous work suggests that behavior of  
249 historical botanists may introduce biases into ecological inferences made from historic collections  
250 (Kozlov et al., 2020). Prolific collectors who contribute thousands of specimens may be more or  
251 less likely to collect certain species, or specimens with certain traits (Daru et al., 2018). Similarly,  
252 the process of scoring seeds for hyphae involved multiple researchers (or "scorers") who, even with  
253 standardized training, may vary in their likelihood of positively identifying *Epichloë*.

254 We performed model fitting using the *inlabru* R package (Bachl et al., 2019). Global intercept  
255 and slope parameters,  $A$  and  $T$ , were given vague priors. Collector and scorer random effects,  $\chi$  and

256  $\omega$  respectively, were centered at 0 with precision parameters assigned penalized complexity (PC) pri-  
257 ors with parameter values  $U_{PC} = 1$  and  $a_{PC} = 0.01$  (Simpson et al., 2017). Each spatially-structured  
258 parameter depended on a covariance matrix according to the proximity of each pair of collection  
259 locations (Bakka et al., 2018; Lindgren et al., 2011). The covariance matrix was approximated using  
260 a Matérn covariance function, with each data point assigned a location according to the nodes of  
261 a mesh of non-overlapping triangles encompassing the study area (Fig. A2). Matérn covariance  
262 functions are widely used in spatially explicit statistical modeling because of their mathematical  
263 tractability and flexibility. This covariance structure relies on the assumption that the underlying  
264 process is stationary and isotropic, such that spatial autocorrelation between data points depends  
265 only on their relative positions (Bakka et al., 2018).

266 Implementing spatially-structured parameters in INLA with this SPDE approach is useful par-  
267 ticularly because space is treated as a continuous variable, allowing the model to make efficient use  
268 of the data and generate predictions across the entire study region. The SPDE approach is flexible  
269 enough that it can capture smooth trends across space that are informed by the data rather than  
270 by spatial regions chosen *a priori* by researchers. However this flexibility also invites the risk of  
271 overfitting, as with other non-linear modeling approaches (Lapeyrolerie and Boettiger, 2023; Ra-  
272 mampiandra et al., 2023; Ward et al., 2014). Priors for the Matérn covariance function, termed  
273 “range” and “variance”, define how proximity effects decay with distance. The choice of priors for  
274 these types of spatial models is an area of active research (Bakka et al., 2018; Simpson et al., 2017),  
275 but another advantage of the INLA approach is that its computational efficiency allows for prior  
276 sensitivity analyses. Results presented in the main text reflect a prior range of 342 kilometers (i.e.  
277 a 50% probability of estimating a range less than 342 kilometers). We tested a range of values  
278 (from 68 kilometers to 1714 kilometers) and meshes (presented in the Supporting Methods – *Mesh*  
279 and *Prior Sensitivity Analysis*), finding that while the magnitude and uncertainty of effects varied,  
280 model results were qualitatively similar, i.e. the same direction of effects across space. We assessed  
281 model fit with visual posterior predictive checks (Fig. A3) and measurements of AUC (Figs. A4-  
282 A5) (Gelman and Hill, 2006). Through results and discussion that follow, we refer to the model

283 described in this section as the “endophyte prevalence model”.

284 *Modeling distributions of host species*

285 The herbarium records did not encompass the entirety of each host species’ range. Therefore, we  
286 used additional data sources to model the geographic distribution of each host species, with two  
287 goals: (1) generate realistic maps on which we could project the predictions of the INLA model,  
288 and (2) use the geographic distributions to test for relationships between climate change drivers and  
289 trends in endophyte prevalence. We followed the ODMAP (overview, data, model, assessment,  
290 prediction) protocol (Crossley et al., 2022) (see Supporting Methods). In short, we used presence-  
291 only observations of each host species from Global Biodiversity Information Facility (GBIF) between  
292 1990 to 2020 (713 occurrence records for *A. hyemalis* (GBIF.Org, 2025a), 656 occurrence records  
293 for *A. perennans* (GBIF.Org, 2025b), and 2338 occurrence records for *E. virginicus* (GBIF.Org,  
294 2025c)). We fit maximum entropy (MaxEnt) models using the maxent function in the R package  
295 *dismo* (Hijmans et al., 2017) using the following seasonal climate predictors (1990-2020 climate  
296 normals): mean and standard deviation of spring, summer, and autumn temperature, and mean  
297 and standard deviation of spring, summer, and autumn cumulative precipitation.

298 We generated 10,000 pseudo-absences as background points, and split the occurrence data into  
299 75% for model training and 25% for model testing. The performance of models was evaluated with  
300 AUC (Jiménez-Valverde, 2012). We found AUC values of 0.862, 0.838, 0.821 respectively for *Agrostis*  
301 *hyemalis*, *Agrostis perennans*, and *Elymus virginicus* indicating good model fit to data. We used  
302 the training sensitivity (true positive rate) and specificity (true negative rate) to set a threshold for  
303 transforming the continuous predicted probabilities into binary presence - absence host distribution  
304 maps on which we projected INLA predictions of endophyte prevalence (Liu et al., 2005).

305

## Assessing the role of climate drivers

306 We assessed how the magnitude of climate change may have driven changes in endophyte prevalence  
307 by assessing correlations between changes in climate and changes in endophyte prevalence predicted  
308 from our spatial model at evenly spaced pixels across the study area.

309 We first downloaded monthly temperature and precipitation rasters from the PRISM climate  
310 group (Daly and Bryant, 2013) covering the time period between 1895 and 2020 using the *prism*  
311 R package (Hart and Bell, 2015). PRISM provides reconstructions of historic climate variables  
312 across the United States by spatially interpolating weather station data (Di Luzio et al., 2008).  
313 Because the magnitude of observed climate change differs across seasons, and because different  
314 growing seasons is a key feature of the biology of our focal host species, we calculated 30-year  
315 climate normals for seasonal mean temperature and cumulative precipitation for the recent (1990  
316 to 2020) and historic (1895 to 1925) periods. We used three four-month seasons within the year  
317 (Spring: January, February, March, April; Summer: May, June, July, August; Autumn: September,  
318 October, November, December). This division of seasons allowed us to quantify differences in  
319 the primary climate change drivers, temperature and precipitation, associated with the two “cool”  
320 seasons, when we expected our focal species to be most active (*A. hyemalis* flowering phenology:  
321 spring; *E. virginicus*: spring and summer; *A. perennans*: autumn). In addition to mean climate  
322 conditions, environmental variability itself can influence population dynamics (Tuljapurkar, 1982)  
323 and changes in variability are a key prediction of climate change models (IPCC, 2021; Stocker et al.,  
324 2013). Therefore, we calculated the standard deviation for each annual and seasonal climate driver  
325 across each 30-year period. We then took the difference between recent and historic periods for the  
326 mean and standard deviation for each climate driver (Figs. A13-A15). All together, we assessed  
327 twelve potential climate drivers: the mean and standard deviation of spring, summer, and autumn  
328 temperature, as well as the mean and standard deviation of spring, summer, and autumn cumulative  
329 precipitation (the same climate covariates used in the MaxEnt models).

330 We then evaluated whether areas that have experienced the greatest changes in endophyte preva-

lence (hotspots of endophyte change) are associated with high degrees of change in climate (hotspots of climate change). To do so, we modeled the fitted, spatially-varying slopes of endophyte change through time ( $\tau_{h,l}$ ) as a linear function of environmental covariates, with a Gaussian error distribution for a set of pixels across each host distribution. The continuous SPDE approach taken from our endophyte prevalence model allows us to generate predictions of temporal trends in prevalence at arbitrarily many pixels across each host distribution. Balancing computation time with resolution, we generated predicted trends for 546, 645, and 753 pixels across each host distribution for *A. perennans*, *A. hyemalis*, and *E. virginicus* respectively (pixel dimensions: *A. perennans* = 65 km x 36 km; *A. hyemalis* = 61km x 45 km; *E. virginicus* = 62 km x 40 km ). Fitting regressions to many pixels across the study region risks artificially inflating confidence in our results due to large sample sizes, and so we performed this analysis using only a random subsample of 250 pixels across the study region; other sizes of subsample yielded similar results. Data from each host species were analyzed separately. Throughout the results and discussion that follow, we refer to this analysis as the “*post hoc* climate regression analysis”.

#### 345 *Validating model performance with in-sample and out-of-sample tests*

346 We evaluated the predictive ability of the endophyte prevalence model using both in-sample training  
347 data from the herbarium surveys, and with out-of-sample test data, an important but rarely used  
348 strategy in ecological studies (Lee et al., 2024; Tredennick et al., 2021). We generated out-of-  
349 sample test data from contemporary surveys of endophyte prevalence in natural populations of *A.*  
*hyemalis* and *E. virginicus* in Texas and the southern US. Surveys of *E. virginicus* were conducted  
351 in 2013 as described in Sneed et al. (2017), and surveys of *A. hyemalis* took place between 2015  
352 and 2020. Population surveys of *A. hyemalis* were initially designed to cover longitudinal variation  
353 in endophyte prevalence towards its range edge, while surveys of *E. virginicus* were designed to  
354 cover latitudinal variation. In total, we visited 43 populations of *A. hyemalis* and 20 populations  
355 of *E. virginicus* across the south-central US, with emphasis on Texas and neighboring states (Fig  
356 A12). number of plants sampled per population: 22.9); note that this sampling design provided

357 greater local depth of information than the herbarium records, where only one plant was sampled at  
358 each locality. We quantified the endophyte status of each individual with microscopy as described  
359 for the herbarium surveys (with 5-10 seeds scored per individual), and calculated the prevalence  
360 of endophytes within the population (proportion of plants that were endophyte-symbiotic). For  
361 each population, we compared the observed fraction of endophyte-symbiotic hosts to the predicted  
362 probability of endophyte occurrence  $\hat{P}$  derived from the model for that location and year. The  
363 contemporary survey period (2013-2020) is at the most recent edge of the time period encompassed  
364 by the historical specimens used for model fitting.

365 **Results**

366 *How has endophyte prevalence changed over time?*

367 Across more than 2300 herbarium specimens dating back to 1824, we found that prevalence of  
368 *Epichloë* endophytes increased over the last two centuries for all three grass host species (Fig. 2).  
369 On average, endophytes of *A. perennans* and *E. virginicus* increased from ~ 40 % to 70% prevalence  
370 across the study region, and *A. hyemalis* increased from ~ 25% to over 50% prevalence. Our model  
371 indicates high confidence that overall temporal trends are positive across species (99% probability  
372 of a positive overall year slope in *A. hyemalis*, 92% probability of a positive overall year slope in *A.*  
373 *perennans*, and 91% probability of a positive overall year slope in *E. virginicus*) (Fig. A6).

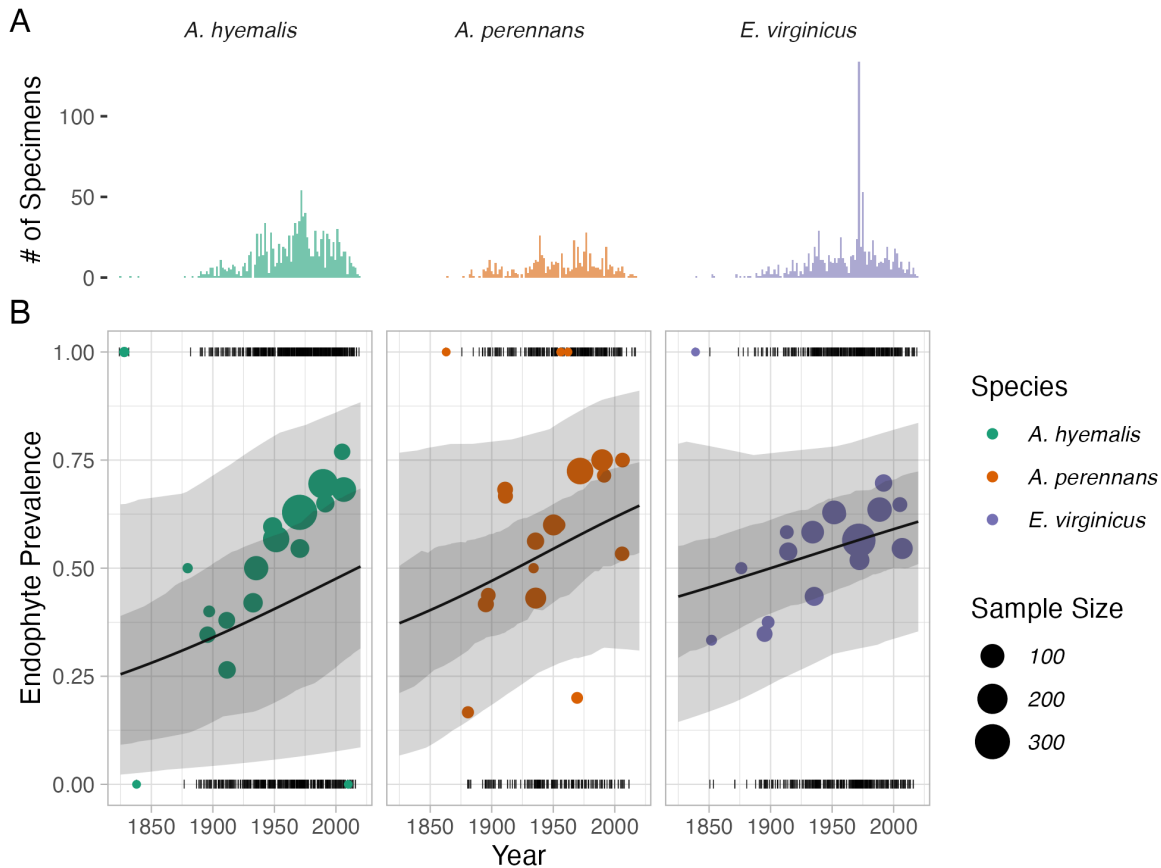


Figure 2: **Temporal trends in endophyte prevalence.** (A) Histograms show the frequency of scored specimens through time for each host species. (B) Lines show mean endophyte prevalence predicted by the endophyte prevalence model over the study period along with the 50% and 95% CI bands incorporating parameter uncertainty and variation associated with collector and scorer random effects. Colored points are binned means of the observed endophyte presence/absence data (black dashes). Colors represent each host species (*A. hyemalis*: green, *A. perennans*: orange, *E. virginicus*: purple) and point size represents the number of specimens.

374 The model appears to under-predict the observed increase in endophyte prevalence relative to  
 375 the data, particularly for *A. hyemalis* (Fig. 2B), but the model is accounting for random effects  
 376 and spatial non-independence that are not readily seen in the figure. We found no evidence that  
 377 collector biases influenced our results. Collector random effects were consistently small (Fig. A9),

378 and models fit with and without this random effect provide qualitatively similar results. The identity  
379 of individual scorers, the researchers who identified endophyte status microscopically, did contribute  
380 to observed patterns in endophyte prevalence. For example, 3 of the 25 scorers were significantly  
381 more likely than average to assign positive endophyte status, as indicated by 95% credible intervals  
382 greater than zero, while 4 of the 25 had 95% credible intervals below zero (Fig. A10).

383 *How spatially variable are temporal trends in endophyte prevalence?*

384 While there was an overall increase in endophyte prevalence, our model revealed hotspots and  
385 coldspots of change across the host species' ranges, which are mapped in Fig. 3 across geographic  
386 ranges predicted by MaxEnt species distribution models. In some regions, posterior mean estimates  
387 of spatially varying temporal trends indicate that *A. hyemalis* and *A. perennans* experienced in-  
388 creases in prevalence by as much as 2% per year over the study period. Posterior estimates of  
389 uncertainty in spatially varying slopes indicate that these hotspots of change may have experienced  
390 increases of up to 5% per year while declines in prevalence may be as great as -4% per year for  
391 the *Agrostis* species. (Fig. A7) In contrast, *E. virginicus* experienced increases up to around 1%  
392 per year, with uncertainty ranging between 3.5% increases and 2.5% decreases (Fig. A7) Taken  
393 together, both *Agrostis* species show areas of both strong increasing and declining prevalence, while  
394 *E. virginicus* had an overall weaker and geographically more homogeneous increase in endophyte  
395 prevalence. Notably, endophytes are predicted to have increased most strongly towards the western  
396 range edge of *A. hyemalis* (Fig. 3A) and across the northeastern US for *A. perennans* (Fig. 3B).  
397 Broad increases in prevalence on average, along with increases towards range edges that had low  
398 historic prevalence result in range expansions of the symbiosis for both *Agrostis* species (Fig. 4).  
399 Increases in prevalence were strongest in regions with low historic prevalence for the *Agrostis* species  
400 (Fig. A11 A-B), but for *E. virginicus* trends did not differ according to historic prevalence (A11  
401 C).

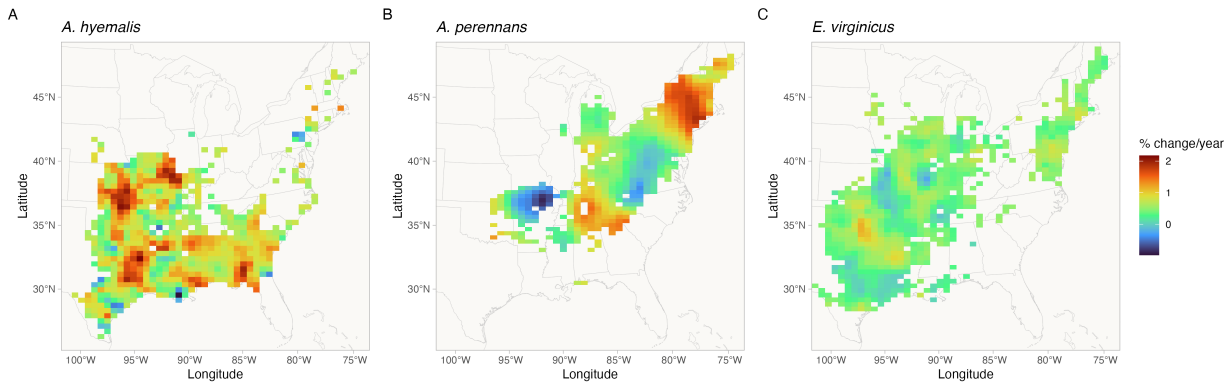


Figure 3: Predicted posterior mean of spatially-varying slopes representing change in endophyte prevalence for each host species ((A) *A. hyemalis*; (B) *A. perennans*; (C) *E. virginicus*). Spatially-varying trends are estimated from the endophyte prevalence model. Color indicates the relative change in predicted endophyte prevalence. Map lines delineate study areas and do not necessarily depict accepted national boundaries.

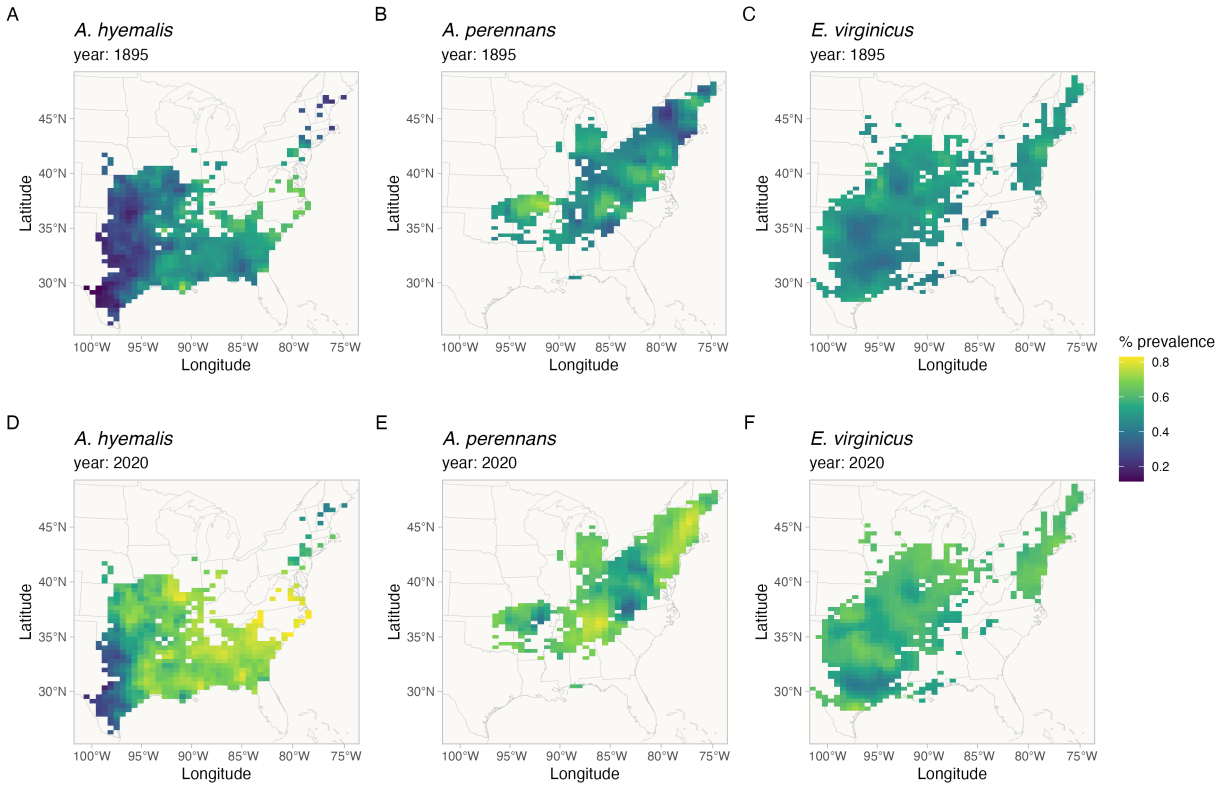


Figure 4: Predicted endophyte prevalence for each host species in 1895 and 2020. Predictions of prevalence come from the endophyte prevalence model. Color indicates the posterior mean endophyte prevalence for (A, D) *A. hyemalis*, (B, E) *A. perennans*, and (C, F) *E. virginicus*. Map lines delineate study areas and do not necessarily depict accepted national boundaries.

402     What is the relationship between variation in temporal trends in endophyte  
403     prevalence and changes in climate drivers?

404     We found that trends in endophyte prevalence were strongly associated with one or more seasonal  
405     climate change drivers (Fig. 5). For the majority of the study region, the climate has become  
406     wetter (an average increase in annual precipitation of 60 mm) with relatively minimal temperature  
407     warming (an average increase in annual temperature of 0.02 °C) over the last century (Fig. A13-  
408     A15), a consequence of regional variation in global climate change (IPCC, 2021). Within the

409 region, climate changes were spatially variable; certain locations experienced increases in annual  
410 precipitation as large as 375 mm or decreases up to 54 mm across the last century, while annual  
411 temperature changes ranged from warming as great as 1.4 °C to cooling by 0.46 °C.

412 Spatially variable climate trends were predictive of trends in endophyte prevalence. For exam-  
413 ple, among the tested climate drivers, strong increases in endophyte prevalence for *A. perennans*  
414 were most strongly associated with increasing autumn precipitation and with increasing mean and  
415 variability in autumn temperature (greater than 97% posterior probabilities of positive slopes). For  
416 this species, each 1 °C increase in autumn temperature was associated with a 1.07 % greater increase  
417 per year in endophyte prevalence (Fig. 5A) and a 100 mm increase in precipitation was associated  
418 with a 0.8% greater increase per year in endophyte prevalence (Fig. 5B). This result aligns with  
419 the species' autumn active growing season, however other seasonal climate drivers were also posi-  
420 tively associated with increasing endophyte prevalence in this host species. In particular, we found  
421 cooler and drier springs and cooler summers to be associated with increasing endophyte prevalence  
422 (greater than 99% posterior probabilities of negative slopes), though these slopes were generally of  
423 smaller magnitude than those for autumn climate drivers. Changes in endophyte prevalence across  
424 the ranges of *A. hyemalis* and *E. virginicus* were less strongly driven by changes in climate. Like  
425 *A. perennans*, climate during peak growing season (spring for *A. perennans* and summer for *E. vir-*  
426 *ginicus*) emerged most commonly as drivers of changes in endophyte prevalence. Across the tested  
427 climate drivers, increases in mean spring precipitation were the strongest predictor of increasing  
428 trends in endophyte prevalence for *A. hyemalis* (Fig. 5B) (greater than 99% posterior probability  
429 of a positive slope). For this species, an increase of 100 mm in spring precipitation was associated  
430 with 0.6% per year stronger increases in endophyte prevalence relative to regions with no change in  
431 precipitation. The next greatest slopes were those associated with variability in spring precipitation  
432 (greater than 96% posterior probability of a negative slope), as well as in the mean and variabil-  
433 ity of autumn climate (greater than 98% probability of negative and positive slopes, respectively).  
434 Changes in endophyte prevalence in *E. virginicus* were not strongly associated with changes in most  
435 climate drivers, but regions with reduced variability in autumn precipitation (Fig. 5B) and with

436 cooler and more variable summer temperatures (Fig. 5A,C) experienced the largest increases in  
437 endophyte prevalence. Our analysis indicated relatively high confidence that these climate drivers  
438 influence endophyte prevalence shifts in *E. virginicus* (greater than 99% posterior probability of ei-  
439 ther negative or positive slopes respectively), however they translate, for example, to less than a  
440 0.4% decrease in endophyte prevalence per year for each  $1^{\circ}C$  of summer warming over the century.  
441 Repeating this analysis using all pixels across each species' distribution were qualitatively similar  
442 to these results.

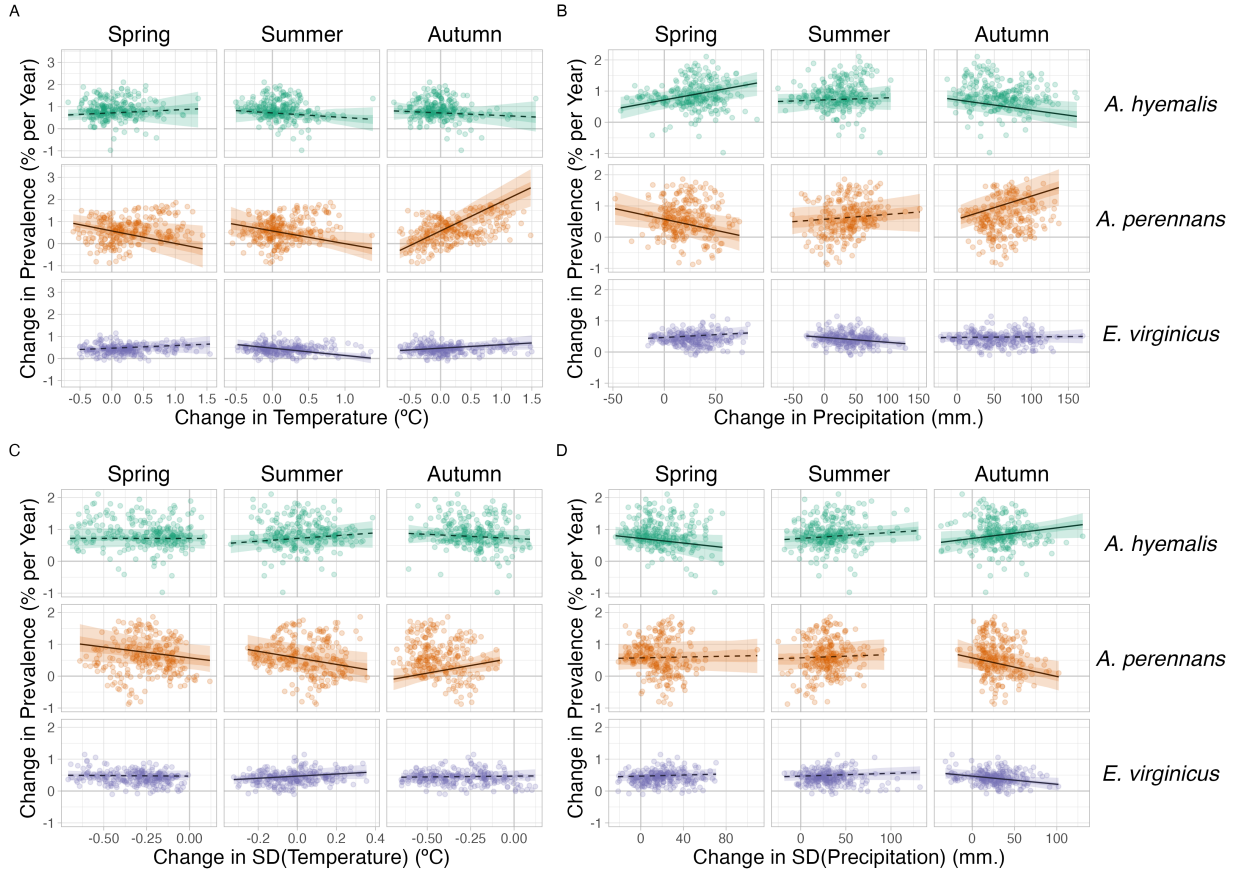


**Figure 5: Relationships between predicted trends in endophyte prevalence and changes in seasonal climate drivers.** Lines show marginal predicted relationship between spatially-varying trends in endophyte prevalence and changes in mean and variability of climate ((A): mean temperature, (B): cumulative precipitation, (C): standard deviation in temperature, (D): standard deviation in precipitation) estimated from the *post hoc* climate regression analysis. Confidence bands represent the 50 and 95% CI, colored by host species (*A. hyemalis*: green, *A. perennans*: orange, *E. virginicus*: purple). Slopes with greater than 95% posterior probability of being either positive or negative are represented as solid lines while those that have less than 95% probability are dashed. Points are the values of pre-computed SVC trends and climate drivers at 250 randomly sampled pixels across each host's distribution used in model fitting for the *post hoc* climate regression analysis.

443

### *Evaluation of model performance on an out-of-sample test*

444 Tests of the endophyte prevalence model's predictive performance, as quantified by AUC and by  
445 visual posterior predictive checks, indicated good predictive ability. Model performance was similar  
446 between historic herbarium specimens used as training data and the out-of-sample test data from  
447 contemporary surveys (AUC = 0.79 and 0.77 respectively; Fig. A5-A4). The model successfully  
448 captured broad regional trends in endophyte prevalence seen in the contemporary survey data,  
449 such as decline endophyte prevalence in *A. hyemalis* towards western longitudes (Fig. 6A) and an  
450 increase towards northern latitudes (Fig. 6B). It is noteable that model predictions for endophyte  
451 prevalence exhibited relatively little local geographic variation, whereas the out-of-sample survey  
452 data were highly variable with populations spanning 0% to 100% endophyte-symbiotic plants (Fig.  
453 6C), indicating population-to-population variation not captured in the endophyte prevalence model.

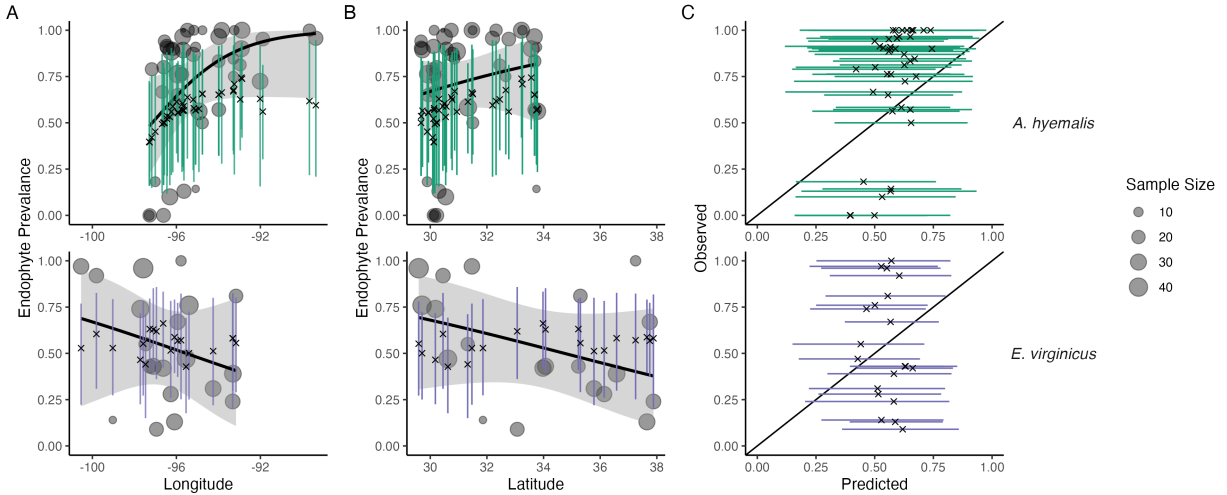


**Figure 6: Predictive performance for contemporary test data.** (A) The endophyte prevalence model, trained on historic herbarium collection data, performed modestly at predicting prevalence in contemporary population surveys. The model captured regional trends across (A) longitude and (B) latitude. Crosses indicate predicted mean prevalence along with the 95% CI (colored lines: *A. hyemalis*: green, orange, *E. virginicus*: purple) from the herbarium model. Contemporary prevalence is represented by grey points (point size reflects sample size) along with trend lines from generalized linear models (black line and shaded 95% confidence interval). (C) Comparison of contemporary observed population prevalence vs. predicted endophyte prevalence shows that contemporary test data had more variance between populations than in model predictions.

## Discussion

Our examination of historic plant specimens revealed previously hidden shifts in microbial symbiosis over the last two centuries. For the three grass host species we examined, there have been strong increases in prevalence of *Epichloë* endophyte symbiosis. We interpret increases in prevalence of *Epichloë*, which are vertically transmitted, as adaptive changes that improve the fitness of their hosts under increasing environmental stress. This interpretation is in line with theory predicting that positive fitness feedback caused by vertical transmission leads beneficial symbionts to rise in

461 prevalence within a population (Donald et al., 2021; Fine, 1975). We further found that trends  
462 in endophyte prevalence often varied across the host distribution in association with changes in  
463 climate drivers, consistent with the hypothesis that increases in endophyte prevalence are driven  
464 by context-dependent benefits to hosts that confer resilience under environmental change. Taken  
465 together, our results suggest an overall strengthening of host-symbiont mutualism over the last two  
466 centuries.

467 *Responses of host-microbe symbioses to climate change*

468 Differences across host species underscore that while all of these  $C_3$  grasses share similar broad-scale  
469 distributions, each engages in unique biotic interactions and has unique responses to environmental  
470 drivers. We identified hotspots of change for *A. perennans*, which was the species whose endophyte  
471 prevalence was most responsive to changes in climate drivers (Fig. 5). Predicted declines of 0.9%  
472 per year in the southern portion of its range and predicted increases of up to 2% per year in the  
473 north suggest a potential poleward range shift of endophyte-symbiotic plants (Fig. 3B); whether  
474 the overall host distribution is shifting in parallel is an exciting next question.

475 Based on previous work demonstrating that endophytes can shield their hosts from drought  
476 stress (reviewed in Decunta et al. (2021)), we generally predicted that drought conditions would be  
477 a driver of increasing endophyte prevalence. In contrast to this expectation, increasing prevalence  
478 for *A. perennans* was associated with both increasing autumn temperature and precipitation (Fig.  
479 5). To our knowledge, the response of the symbiosis in *A. perennans* to drought has not been  
480 examined experimentally, but in a greenhouse experiment, endophytes had a positive effect on host  
481 reproduction under shaded, low-light conditions (Davitt et al., 2010). Our results also hint that it  
482 may be useful to investigate whether lagged climate effects are important predictors of host fitness  
483 in this system (Evers et al., 2021). Endophyte prevalence of the autumn-flowering *A. perennans* was  
484 strongly linked with decreasing spring precipitation, and that of the spring-flowering *A. hyemalis*  
485 was associated with decreasing autumn precipitation (Fig. 5B). For *A. hyemalis*, endophytes could  
486 be playing a role helping hosts weather autumn-season droughts, which is likely also an important

487 time for the species' germination. Previous work demonstrated drought benefits in a greenhouse  
488 manipulation with this host-symbiont pair (Davitt et al., 2011), and early life stages may be partic-  
489 ularly vulnerable to prolonged droughts. For *E. virginicus*, which experienced the weakest changes  
490 in endophyte prevalence overall (ranging between 1.1% increases and 0.2% decreases), we only found  
491 modest associations with changes in climate drivers. Surveys by Sneek et al. (2017), used as part  
492 of the test data in this study, identified a drought index (SPEI) that integrates precipitation with  
493 estimated evapotranspiration as an important predictor of contemporary endophyte prevalence in  
494 this species. The diverse relationships we detect between trends in endophyte prevalence and cli-  
495 mate drivers suggest a more complicated picture than the simple explanation that drought alone, as  
496 measured through changes in annual precipitation, causes increasing endophyte prevalence through  
497 context-dependent fitness benefits.

498 While we show consistent increasing trends in prevalence between the three species, the mecha-  
499 nisms that explain these changes may be diverse and idiosyncratic. First, climate change responses  
500 may depend on genotype-specific responses that are not considered in our current analysis. While  
501 *Epichloë* symbioses are highly specialized, surveys have demonstrated genotypic and chemotypic  
502 diversity of the symbionts among and within populations (Treindl et al., 2023; von Cräutlein et al.,  
503 2021). Genotypic variation in *Epichloë* endophytes, particularly in genes responsible for alkaloid  
504 production, produces "chemotypes" with differing benefits for hosts against insect or mammalian  
505 herbivores mediated by environmental conditions (Saikkonen et al., 2013; Schardl et al., 2012).  
506 Genotypic variation of the hosts themselves can also influence interaction outcomes (Gundel et al.,  
507 2011; Parker et al., 2017). Whether hotspots of change in endophyte prevalence reflect selection for  
508 genotype-pairings with particularly strong fitness benefits is an unanswered question. Additionally,  
509 *Epichloë* endophytes have been connected to a suite of non-drought related fitness benefits includ-  
510 ing herbivory defense (Brem and Leuchtmann, 2001), salinity resistance (Wang et al., 2020), and  
511 mediation of pathogens (Vikuk et al., 2019) and the soil microbiome (Roberts and Ferraro, 2015).  
512 Broad changes in the distribution and abundance of natural enemies (Côté et al., 2004), along with  
513 stresses from anthropogenic changes in land management and pollution (Sage, 2020) likely influence

514 the benefits of symbiosis (Rudgers et al., 2020). Changing endophyte prevalence results from the  
515 combination of net fitness benefits playing out across the heterogeneous map of a changing climate  
516 and its interactive effects on other anthropogenic drivers. Host species experience a world that  
517 is made increasingly stressful by a combination of global change drivers, and while historic trends  
518 that we observed suggest that symbiotic fitness benefits have helped mitigate this stress, it is pos-  
519 sible that at yet higher levels of stress, increasing costs of the mutualism could lead to declines in  
520 endophyte prevalence. More extreme climate stresses, which are expected more frequently in the  
521 future (Seneviratne et al., 2021) could shift the balance of interactions costs and benefits. Identify-  
522 ing ‘tipping points’ of mutualism breakdown under increasing environmental stress is an important  
523 area of future inquiry.

524 Our results indicate that *Epichloë* symbiosis has likely improved host fitness in stressful en-  
525 vironments leading to increasing prevalence. What is less clear is how this will influence future  
526 range shifts. Based on our analysis, it is likely that the symbiosis will facilitate range shifts for  
527 hosts by improving population growth at range edges. Previous population surveys (Rudgers and  
528 Swafford, 2009; Semmarin et al., 2015; Sneck et al., 2017) attributed environment-dependent gra-  
529 dients in endophyte prevalence to symbiont-derived fitness benefit’s allowing hosts to persist in  
530 environments where they otherwise could not (Afkhami et al., 2014; Kazenel et al., 2015). However,  
531 symbiont-facilitated range shifts require that endophytes be present in the populations to be able  
532 to contribute to population growth. For example, the arid western range edge of *A. hyemalis* has  
533 had historically low endophyte prevalence (Fig. 4), and while prevalence has increased most quickly  
534 in regions with historically low endophyte prevalence (Fig. A11), the complete absence of endo-  
535 phytes at range edges in this species would make it impossible for prevalence to increase without  
536 dispersal of symbiotic seeds (Fowler et al., 2023). These factors potentially contribute to the ability  
537 of the host species to track its environmental niche. Another interesting question is the degree to  
538 which symbiotic and non-symbiotic hosts, which occupy overlapping but distinct niches, are likely  
539 to experience distribution shifts in tandem or at different rates in the future.

540 *Steps towards forecasts of host-microbe symbioses*

541 The combination of a spatially-explicit model and historic herbarium specimens allowed us  
542 to identify regions of both increasing and decreasing endophyte prevalence. We see several next  
543 steps toward the goal of predicting host and symbiont niche-shifts in response to future climate  
544 change. While the model successfully predicted large-scale spatial trends observed in the out-  
545 of-sample contemporary population surveys, these data contained more population-to-population  
546 variability in prevalence than could be explained by the model. We interpret this to mean that  
547 the model captures coarse-scale spatial and temporal trends reasonably well, but is not equipped  
548 to capture local-scale nuances that generate population-to-population differences. Validating our  
549 model predictions with this test, a rare extra step in collections-based studies, allows us to identify  
550 ways in which the model's out-of-sample predictive ability could be improved. Lack of information  
551 on local variability in symbiont prevalence may simply be a feature of data derived from herbarium  
552 specimens. Natural history collectors sample one or a few specimens from local populations, and  
553 these observations are aggregated by the model to derive broad-scale estimates. This suggests that  
554 increasing local replication should be a factor considered in future collection efforts of natural history  
555 specimens, balancing the required time and effort along with limitations on storage space within  
556 collections. Herbarium collections were predominately used for taxonomic research in the past,  
557 but use of specimens to understand ongoing global change would benefit from increased collection  
558 efforts and expansion of herbarium collections. An alternative validation test would be to hold-out  
559 samples from the historic data set. Such a test would more clearly match the conditions of the  
560 training data (i.e., in spatial scale and climate conditions), however the trade-off between training  
561 and testing the model with a limited number of sampled specimens held us back from exploring this  
562 option. Splitting datasets can negatively impact model estimates, and the choice of how to split  
563 the data for model validation is not trivial (Bergmeir and Benítez, 2012; James et al., 2013).

564 Another key consideration in forecasting the dynamics of host-microbe symbioses is the spatial  
565 scale of both specimen georeferencing and available climate data. For this analysis, most specimen

566 localities were assigned coordinates at county or city centroids, and the climate data examined  
567 was on 4 km grid cells. Georeferencing of specimens as accurately as possible is a key priority  
568 of herbarium specimen digitization efforts (Davis, 2023; Soltis, 2017). While the INLA modeling  
569 approach that we used allows for predictions at arbitrarily small spatial scales, and would simplify  
570 connecting model predictions to the scale of a given climate driver, the coarse scale inherent to our  
571 analysis may obscure some local-scale ecological processes. Poor predictive ability at local scales in  
572 this grass-endophyte system is not surprising, as previous studies have found that local variation  
573 (e.g., in soil conditions, in microclimate), even to the scale of hundreds of meters can structure  
574 endophyte-host niches (Gundel et al., 2024; Kazenel et al., 2015). Local adaptation in either the  
575 host or symbiont to microclimate or soil conditions could cause populations to differ from broad  
576 regional trends. The choice of prior distributions for spatially-varying random effects also impacts  
577 the model's flexibility to capture spatial trends. Our exploration of model sensitivity to prior choice  
578 (presented in the *Supplemental Methods*) reveals qualitatively similar results across a broad range  
579 of priors. An important next step would be integrating data from local and regional scales through  
580 modeling to constrain estimates of local and regional variation.

581 Predicting future niche-shifts of hosts and symbionts will require considering the coupled dynam-  
582 ics of host-symbiont dispersal in addition to fitness benefits. For example, transplanting symbiotic  
583 and non-symbiotic plants beyond the range edge of *A. hyemalis* could tell us whether low endophyte  
584 prevalence in that area (Fig. 4A) is a result of environmental conditions that lead the symbiosis  
585 to have negative fitness consequences, or is a result of some historical contingency or dispersal lim-  
586 itation that has thus far limited the presence of symbiotic hosts from a region where they would  
587 otherwise flourish and provide resilience. Incorporating available climatic and soil layers as covari-  
588 ates is another obvious step that could improve predictions. These steps will bridge gaps that often  
589 exist between large but broad bioclimatic and biodiversity data and small but high-resolution data  
590 on biotic interactions, and move towards the goal of predicting the dynamics of microbial symbioses  
591 under climate change (Isaac et al., 2020; Miller et al., 2019).

592 *Herbaria for global change research*

593 Our analysis advances the use of herbarium specimens in global change biology in two ways.  
594 First and foremost, this is one of a growing number of studies to examine microbial symbiosis  
595 using specimens from natural history collections, and the first, to our knowledge, to link long-term  
596 changes in symbioses to changes in climate. The responses of microbial symbioses are a rich target  
597 for future studies within historic specimens, particularly those that take advantage of advances  
598 in sequencing technology. While we used relatively coarse presence/absence data based on fungal  
599 morphology, other studies have examined historic plant microbiomes using molecular sequencing  
600 and sophisticated bioinformatics techniques, but these studies have so far been limited to relatively  
601 few specimens at limited spatial extents (Bearchell et al., 2005; Bieker et al., 2020; Bradshaw et al.,  
602 2021, 2023; Gross et al., 2021; Heberling and Burke, 2019; Yoshida et al., 2015). Much of this work  
603 highlights the important role that historic specimens can play in tracking pathogens, a particularly  
604 important area as climate change facilitates the spread of new diseases (Ristaino, 2020; Singh et al.,  
605 2023) Continued advances in capturing historic DNA and in filtering out potential contamination  
606 during specimen storage (Bakker et al., 2020; Daru et al., 2019; Raxworthy and Smith, 2021) will  
607 be imperative in the effort to scale up these efforts. This scaling up will be essential to be able  
608 to quantify changes not just in the prevalence of symbionts, but also in symbionts' intraspecific  
609 variation and evolutionary responses to climate change, as well as in changes in the wider host  
610 microbiome. With improved molecular insights from historic specimens, we could ask whether  
611 the broad increases in endophytes that we have identified reflect selection for particular genetic  
612 strains or chemotypes and how this selection varies across space. Answering these questions as well  
613 as the unknown questions that future researchers may ask also reiterates the value in capturing  
614 meta-information during ongoing digitization efforts at herbaria around the world and during the  
615 accession of newly collected specimens (Edwards et al.; Lendemer et al., 2020).

616 The second major advance in this analysis is in accounting for several potential biases in the data  
617 observation process that may be common to many collections-based research questions by using a

618 spatially-explicit random effects model. Potential biases introduced by the sampling habits of col-  
619 lectors (Daru et al., 2018), and variation between contemporary researchers during the collection of  
620 trait data, if not corrected for could lead to over-confident inference about the strength and direction  
621 of historic change (Fig. 2). Previous studies that have quantified the effects of collector biases typ-  
622 ically find them to be small (Davis et al., 2015; Meineke et al., 2019), and we similarly did not find  
623 that collector has a strong effect on the results of our analysis, but that scorer identity did impact  
624 results. It is difficult to distinguish whether the impact of scorers was driven by true differences  
625 in scorers' biases or by unintended spatial or temporal clustering of the specimens examined by  
626 each scorer (Clayton et al., 1993; Urdangarin et al., 2023). By under-weighting endophyte-positive  
627 samples that are clustered spatially or by collector or observer, the endophyte prevalence model is  
628 appropriately accounting for nuisance variables and providing a conservative inference of endophyte  
629 change relative to the raw data. Spatial autocorrelation is another phenomenon likely common  
630 in data derived from herbarium specimens (Willems et al., 2022), which our spatially-explicit anal-  
631 ysis models among samples. Beyond spatial autocorrelation of outcomes, systematic differences in  
632 sampling across space can result in spatial bias.

633 One strength of herbaria as vehicles for global change research is the relative ease with which  
634 specimens from many distinct geographic locations can be examined. We visited just nine institu-  
635 tions in the central southern United States, and we were able to sample seeds from specimens across  
636 an area spanning over 300,000 sq. km, including specimens from Mexico and Canada. Despite this  
637 advantage, the specimens we examined are concentrated in the south-central United States, with  
638 fewer specimens in the rapidly warming northeastern United States reflecting the regional focus of  
639 herbaria. We provide a simulation analysis exploring the potential impact of spatially and tempo-  
640 rally biased sampling (Appendix A - Supporting Methods). We found that the spatially-varying  
641 coefficient model had a strong ability to re-capitulate temporal trends across space in simulated  
642 data, and that this result was robust to relatively high levels of spatial bias (80% of data missing  
643 from one spatial region). Simulation analyses that extend this work to consider the myriad ways  
644 herbarium data may be biased (i.e. testing different spatial arrangements and scales of spatial

645 bias, or testing different sample sizes) would be extremely valuable (Daru et al., 2018; Erickson and  
646 Smith, 2021; Gaul et al., 2020; Meineke and Daru, 2021; Schmidt et al.).

647 *Conclusion*

648 Ultimately, a central goal of global change biology is to generate predictive insights into the future of  
649 natural systems on a rapidly changing planet. Beyond host-microbe symbioses, detecting ecological  
650 responses to anthropogenic global change and attributing their causes would inform public policy  
651 decision-makers and adaptive management strategies. Natural history specimens, such as the plant  
652 hosts examined in this study, have a clear role to play in informing global change biodiversity  
653 science, including building understanding of the dynamics of host-symbiont interactions (Davis,  
654 2023). This survey of historic endophyte prevalence is necessarily correlative, yet it serves as a  
655 foundation to develop better predictive models of the response of microbial symbioses to climate  
656 change. Combining the insights from this type of regional-scale survey with field experiments and  
657 physiological performance data could be invaluable to identify mechanisms driving shifts in host-  
658 symbiont dynamics. Evidence is strong that certain dimensions of climate change correlated with  
659 endophytes' temporal responses, however we do not know why trends in prevalence were weak  
660 in some areas or how endophytes would respond to more extreme changes in climate. The "time  
661 machine" of natural history collections revealed evidence of mutualism resilience for grass-endophyte  
662 symbioses in the face of environmental change, but more extreme changes could potentially push  
663 one or both partners beyond their physiological limits, leading to the collapse of the mutualism;  
664 more research is needed to understand what those limits might be.

665 **Acknowledgments**

666 We thank Dr. Jessica Budke for help in drafting our initial destructive sampling plan, and to the  
667 many staff members of herbaria who facilitated our research visits, as well as to the hundreds of  
668 collectors who contributed to the natural history collections. Several high school and undergraduate  
669 researchers contributed to data collection, including A. Appio-Riley, P. Bilderback, E. Chong, K.

670 Dickens, L. Dufresne, B. Gutierrez, A. Johnson, S. Linder, E. Scales, B. Scherick, K. Schrader, E.  
671 Segal , G. Singla, and M. Tucker. This research was supported by funding from National Science  
672 Foundation (grants 1754468 and 2208857) and by funding from the Texas Ecolab Program. Four  
673 anonymous reviewers greatly improved earlier versions of this manuscript.

674 **Statement of Authorship**

675 J.C.F. contributed to research conception, data collection, data analysis, and led manuscript draft-  
676 ing. J.M. contributed to data analysis and manuscript revisions. T.E.X.M. contributed to research  
677 conception, data collection, data analysis, and manuscript revisions.

678 **Data and Code Availability**

679 Data from this publication can be found through a publicly available repository  
680 (<https://doi.org/10.5061/dryad.rn8pk0pn0>). Code for analyses can be found through a publicly  
681 available repository (<https://github.com/joshuacfowler/EndoHerbarium>) that will be permanently  
682 archived upon publication.

## Literature Cited

- 684 M E Afkhami. Fungal endophyte–grass symbioses are rare in the California floristic province and  
685 other regions with mediterranean-influenced climates. *Fungal Ecology*, 5(3):345–352, 2012.
- 686 M E Afkhami and J A Rudgers. Symbiosis lost: Imperfect vertical transmission of fungal endophytes  
687 in grasses. *The American Naturalist*, 172(3):405–416, 2008.
- 688 M E Afkhami, P J McIntyre, and S Y Strauss. Mutualist-mediated effects on species’ range limits  
689 across large geographic scales. *Ecology Letters*, 17(10):1265–1273, 2014.
- 690 S N Aitken, S Yeaman, J A Holliday, T Wang, and S Curtis-McLane. Adaptation, migration  
691 or extirpation: Climate change outcomes for tree populations. *Evolutionary Applications*, 1(1):  
692 95–111, 2008.
- 693 C E Aslan, E S Zavaleta, B Tershy, and D Croll. Mutualism disruption threatens global plant  
694 biodiversity: a systematic review. *PloS one*, 8(6):e66993, 2013.
- 695 F E Bachl, F Lindgren, D L Borchers, and J B Illian. inlabru: an R package for Bayesian spatial  
696 modelling from ecological survey data. *Methods in Ecology and Evolution*, 10(6):760–766, 2019.
- 697 C W Bacon and J F White. Stains, media, and procedures for analyzing endophytes. In *Biotech-  
698 nology of endophytic fungi of grasses*, pages 47–56. CRC Press, 2018.
- 699 H Bakka, H Rue, G-A Fuglstad, A Riebler, D Bolin, J Illian, E Krainski, D Simpson, and F Lind-  
700 gren. Spatial modeling with r-inla: A review. *Wiley Interdisciplinary Reviews: Computational  
701 Statistics*, 10(6):e1443, 2018.
- 702 F T Bakker, V C Bieker, and M D Martin. Herbarium collection-based plant evolutionary genetics  
703 and genomics. *Frontiers in Ecology and Evolution*, 8:603948, 2020.
- 704 D R Bazely, J P Ball, M Vicari, A J Tanentzap, M Bérenger, T Rakocevic, and S Koh. Broad-

- 705 scale geographic patterns in the distribution of vertically-transmitted, asexual endophytes in four  
706 naturally-occurring grasses in sweden. *Ecography*, 30(3):367–374, 2007.
- 707 Sarah J Bearchell, Bart A Fraaije, Michael W Shaw, and Bruce DL Fitt. Wheat archive links long-  
708 term fungal pathogen population dynamics to air pollution. *Proceedings of the National Academy  
709 of Sciences*, 102(15):5438–5442, 2005.
- 710 J Beguin, S Martino, H Rue, and S G Cumming. Hierarchical analysis of spatially autocorrelated  
711 ecological data using integrated nested laplace approximation. *Methods in Ecology and Evolution*,  
712 3(5):921–929, 2012.
- 713 C S Berg, J L Brown, and J J Weber. An examination of climate-driven flowering-time shifts at  
714 large spatial scales over 153 years in a common weedy annual. *American Journal of Botany*, 106  
715 (11):1435–1443, 2019.
- 716 Christoph Bergmeir and José M Benítez. On the use of cross-validation for time series predictor  
717 evaluation. *Information Sciences*, 191:192–213, 2012.
- 718 V C Bieker, F Sánchez Barreiro, J A Rasmussen, M Brunier, N Wales, and M D Martin. Metage-  
719 nomic analysis of historical herbarium specimens reveals a postmortem microbial community.  
720 *Molecular Ecology Resources*, 20(5):1206–1219, 2020.
- 721 J L Blois, P L Zarnetske, M C Fitzpatrick, and S Finnegan. Climate change and the past, present,  
722 and future of biotic interactions. *Science*, 341(6145):499–504, 2013.
- 723 M Bradshaw, U Braun, M Elliott, J Kruse, S-Y Liu, G Guan, and P Tobin. A global genetic analysis  
724 of herbarium specimens reveals the invasion dynamics of an introduced plant pathogen. *Fungal  
725 Biology*, 125(8):585–595, 2021.
- 726 Michael J Bradshaw, Julie Carey, Miao Liu, Holly P Bartholomew, Wayne M Jurick, Sarah Hamble-  
727 ton, Dylan Hendricks, Martin Schnittler, and Markus Scholler. Genetic time traveling: sequenc-  
728 ing old herbarium specimens, including the oldest herbarium specimen sequenced from kingdom

- fungi, reveals the population structure of an agriculturally significant rust. *New Phytologist*, 237(4):1463–1473, 2023.
- D Brem and A Leuchtmann. *Epichloë* grass endophytes increase herbivore resistance in the woodland grass *Brachypodium sylvaticum*. *Oecologia*, 126(4):522–530, 2001.
- T A Carleton and S M Hsiang. Social and economic impacts of climate. *Science*, 353(6304):aad9837, 2016.
- S Cheng, Y-N Zou, K Kuča, A Hashem, E F Abd\_Allah, and Q-S Wu. Elucidating the mechanisms underlying enhanced drought tolerance in plants mediated by arbuscular mycorrhizal fungi. *Frontiers in Microbiology*, 12:4029, 2021.
- K Clay and C Schardl. Evolutionary origins and ecological consequences of endophyte symbiosis with grasses. *The American Naturalist*, 160(S4):S99–S127, 2002.
- D G Clayton, L Bernardinelli, and C Montomoli. Spatial correlation in ecological analysis. *International Journal of Epidemiology*, 22(6):1193–1202, 1993.
- S D Côté, T P Rooney, J-P Tremblay, C Dussault, and D M Waller. Ecological impacts of deer overabundance. *Annu. Rev. Ecol. Evol. Syst.*, 35(1):113–147, 2004.
- KD Craven, PTW Hsiau, A Leuchtmann, W Hollin, and CL Schardl. Multigene phylogeny of *Epichloë* species, fungal symbionts of grasses. *Annals of the Missouri Botanical Garden*, pages 14–34, 2001.
- K M Crawford, J M Land, and J A Rudgers. Fungal endophytes of native grasses decrease insect herbivore preference and performance. *Oecologia*, 164:431–444, 2010.
- M S Crossley, T D Meehan, M D Moran, J Glassberg, W E Snyder, and A K Davis. Opposing global change drivers counterbalance trends in breeding North American monarch butterflies. *Global Change Biology*, 28(15):4726–4735, 2022.

- 752 C Daly and K Bryant. The PRISM climate and weather system — An introduction. *Corvallis, OR:*  
753 *PRISM climate group*, 2, 2013.
- 754 B H Daru, D S Park, R B Primack, C G Willis, D S Barrington, T J S Whitfeld, T G Seidler, P W  
755 Sweeney, D R Foster, A M Ellison, et al. Widespread sampling biases in herbaria revealed from  
756 large-scale digitization. *New Phytologist*, 217(2):939–955, 2018.
- 757 B H Daru, E A Bowman, D H Pfister, and A E Arnold. A novel proof of concept for capturing  
758 the diversity of endophytic fungi preserved in herbarium specimens. *Philosophical Transactions  
759 of the Royal Society B*, 374(1763):20170395, 2019.
- 760 C C Davis, C G Willis, B Connolly, C Kelly, and A M Ellison. Herbarium records are reliable sources  
761 of phenological change driven by climate and provide novel insights into species' phenological  
762 cueing mechanisms. *American Journal of Botany*, 102(10):1599–1609, 2015.
- 763 Charles C Davis. The herbarium of the future. *Trends in Ecology & Evolution*, 38(5):412–423, 2023.
- 764 A J Davitt, M Stansberry, and H A Rudgers. Do the costs and benefits of fungal endophyte symbiosis  
765 vary with light availability? *New Phytologist*, 188(3):824–834, 2010.
- 766 A J Davitt, C Chen, and J A Rudgers. Understanding context-dependency in plant–microbe sym-  
767 biosis: The influence of abiotic and biotic contexts on host fitness and the rate of symbiont  
768 transmission. *Environmental and Experimental Botany*, 71(2):137–145, 2011.
- 769 F A Decunta, L I Pérez, D P Malinowski, M A Molina-Montenegro, and P E Gundel. A systematic  
770 review on the effects of *Epichloë* fungal endophytes on drought tolerance in cool-season grasses.  
771 *Frontiers in Plant Science*, 12:644731, 2021.
- 772 M Di Luzio, G L Johnson, C Daly, J K Eischeid, and J G Arnold. Constructing retrospective  
773 gridded daily precipitation and temperature datasets for the conterminous United States. *Journal  
774 of Applied Meteorology and Climatology*, 47(2):475–497, 2008.

- 775 M L Donald, T F Bohner, K M Kolis, R A Shadow, J A Rudgers, and TEX Miller. Context-  
776 dependent variability in the population prevalence and individual fitness effects of plant–fungal  
777 symbiosis. *Journal of Ecology*, 109(2):847–859, 2021.
- 778 AE Douglas. Host benefit and the evolution of specialization in symbiosis. *Heredity*, 81(6):599–603,  
779 1998.
- 780 Y-W Duan, H Ren, T Li, L-L Wang, Z-Q Zhang, Y-L Tu, and Y-P Yang. A century of pollination  
781 success revealed by herbarium specimens of seed pods. *New Phytologist*, 224(4):1512–1517, 2019.
- 782 E J Edwards, B D Mishler, and C D Davis. University herbaria are uniquely important. *Trends in  
783 Plant Science*.
- 784 M Engel, T Mette, and W Falk. Spatial species distribution models: Using Bayes inference with  
785 INLA and SPDE to improve the tree species choice for important European tree species. *Forest  
786 Ecology and Management*, 507:119983, 2022.
- 787 K D Erickson and A B Smith. Accounting for imperfect detection in data from museums and herbaria  
788 when modeling species distributions: combining and contrasting data-level versus model-level bias  
789 correction. *Ecography*, 44(9):1341–1352, 2021.
- 790 S M Evers, T M Knight, D W Inouye, TEX Miller, R Salguero-Gómez, A M Iler, and A Compagnoni.  
791 Lagged and dormant season climate better predict plant vital rates than climate during the  
792 growing season. *Global Change Biology*, 27(9):1927–1941, 2021.
- 793 P E M Fine. Vectors and vertical transmission: an epidemiologic perspective. *Annals of the New  
794 York Academy of Sciences*, 266(1):173–194, 1975.
- 795 J C Fowler, M L Donald, J L Bronstein, and TEX Miller. The geographic footprint of mutualism:  
796 How mutualists influence species’ range limits. *Ecological Monographs*, 93(1):e1558, 2023.
- 797 J C Fowler, S Ziegler, K D Whitney, J A Rudgers, and TEX Miller. Microbial symbionts buffer

- 798 hosts from the demographic costs of environmental stochasticity. *Ecology Letters*, 27(5):e14438,  
799 2024.
- 800 PR Fraude, F De Jongh, F Vermeulen, J Van Bleijswijk, and RPM Bak. Variation in symbiont  
801 distribution between closely related coral species over large depth ranges. *Molecular Ecology*, 17  
802 (2):691–703, 2008.
- 803 M E Frederickson. Mutualisms are not on the verge of breakdown. *Trends in Ecology & Evolution*,  
804 32(10):727–734, 2017.
- 805 W Gaul, D Sadykova, H J White, L Leon-Sanchez, P Caplat, M C Emmerson, and J M Yearsley.  
806 Data quantity is more important than its spatial bias for predictive species distribution modelling.  
807 *PeerJ*, 8:e10411, 2020.
- 808 GBIF.Org. Occurrence download, 2025a. URL <https://www.gbif.org/occurrence/download/>  
809 0018831-250127130748423.
- 810 GBIF.Org. Occurrence download, 2025b. URL <https://www.gbif.org/occurrence/download/>  
811 0018850-250127130748423.
- 812 GBIF.Org. Occurrence download, 2025c. URL <https://www.gbif.org/occurrence/download/>  
813 0018851-250127130748423.
- 814 A Gelman and J Hill. *Data analysis using regression and multilevel/hierarchical models*. Cambridge  
815 University Press, 2006.
- 816 S E Gilman, M C Urban, J Tewksbury, G W Gilchrist, and R D Holt. A framework for community  
817 interactions under climate change. *Trends in Ecology & Evolution*, 25(6):325–331, 2010.
- 818 G Granath, M Vicari, D R Bazely, J P Ball, A Puentes, and T Rakocevic. Variation in the abundance  
819 of fungal endophytes in fescue grasses along altitudinal and grazing gradients. *Ecography*, 30(3):  
820 422–430, 2007.

- 821 A Gross, C Petitcollin, C Dutech, B Ly, M Massot, J Faivre d'Arcier, L Dubois, G Saint-Jean, and  
822 M-L Desprez-Loustau. Hidden invasion and niche contraction revealed by herbaria specimens  
823 in the fungal complex causing oak powdery mildew in europe. *Biological Invasions*, 23:885–901,  
824 2021.
- 825 P E Gundel, I Zabalgogeazcoa, and BRV De Aldana. Interaction between plant genotype and  
826 the symbiosis with *Epichloë* fungal endophytes in seeds of red fescue (*Festuca rubra*). *Crop and*  
827 *Pasture Science*, 62(11):1010–1016, 2011.
- 828 P E Gundel, A C Ueno, C Casas, TEX Miller, L I Pérez, R Cuyeu, and M Omacini. Temporal  
829 host–symbiont dynamics in community contexts: Impacts of host fitness and vertical transmission  
830 efficiency on symbiosis prevalence. *Functional Ecology*, 38(12):2610–2622, 2024.
- 831 E K Hart and K Bell. *prism: Download data from the Oregon prism project*, 2015. URL <https://github.com/ropensci/prism>. R package version 0.0.6.
- 832
- 833 J J Heberling and D J Burke. Utilizing herbarium specimens to quantify historical mycorrhizal  
834 communities. *Applications in plant sciences*, 7(4):e01223, 2019.
- 835 R J Hijmans, S Phillips, J Leathwick, J Elith, and Robert J Hijmans. Package ‘dismo’. *Circles*, 9  
836 (1):1–68, 2017.
- 837 J HilleRisLambers, M A Harsch, A K Ettinger, K R Ford, and E J Theobald. How will biotic  
838 interactions influence climate change-induced range shifts? *Annals of the New York Academy of*  
839 *Sciences*, 1297(1):112–125, 2013.
- 840 IPCC. Climate change 2021: The physical science basis, 2021. URL <https://www.ipcc.ch/report/ar6/wg1/>.
- 841
- 842 N J B Isaac, M A Jarzyna, P Keil, L I Damblby, P H Boersch-Supan, E Browning, S N Freeman,  
843 N Golding, G Guillera-Arroita, P A Henrys, et al. Data integration for large-scale models of  
844 species distributions. *Trends in Ecology & Evolution*, 35(1):56–67, 2020.

- 845 Gareth James, Daniela Witten, Trevor Hastie, Robert Tibshirani, et al. *An introduction to statistical*  
846 *learning*, volume 112. Springer, 2013.
- 847 A Jiménez-Valverde. Insights into the area under the receiver operating characteristic curve (auc)  
848 as a discrimination measure in species distribution modelling. *Global Ecology and Biogeography*,  
849 21(4):498–507, 2012.
- 850 D Kahle and H Wickham. Package ‘ggmap’. *Retrieved September*, 5:2021, 2019.
- 851 M R Kazenel, C L Debban, L Ranelli, W Q Hendricks, Y A Chung, T H Pendergast IV, N D  
852 Charlton, C A Young, and J A Rudgers. A mutualistic endophyte alters the niche dimensions of  
853 its host plant. *AoB plants*, 7:plv005, 2015.
- 854 R A Knapp, G M Fellers, P M Kleeman, D AW Miller, V T Vredenburg, E B Rosenblum, and C J  
855 Briggs. Large-scale recovery of an endangered amphibian despite ongoing exposure to multiple  
856 stressors. *Proceedings of the National Academy of Sciences*, 113(42):11889–11894, 2016.
- 857 M V Kozlov, I V Sokolova, V Zverev, A A Egorov, M Y Goncharov, and E L Zvereva. Biases in  
858 estimation of insect herbivory from herbarium specimens. *Scientific Reports*, 10(1):12298, 2020.
- 859 Marcus Lapeyrolerie and Carl Boettiger. Limits to ecological forecasting: Estimating uncertainty  
860 for critical transitions with deep learning. *Methods in Ecology and Evolution*, 14(3):785–798, 2023.
- 861 B R Lee, E F Alecrim, T K Miller, J RK Forrest, J M Heberling, R B Primack, and R D Sargent.  
862 Phenological mismatch between trees and wildflowers: Reconciling divergent findings in two recent  
863 analyses. *Journal of Ecology*, 112(6):1184–1199, 2024.
- 864 J Lendemer, B Thiers, A K Monfils, J Zaspel, E R Ellwood, A Bentley, K LeVan, J Bates, D Jen-  
865 nings, D Contreras, et al. The extended specimen network: A strategy to enhance us biodiversity  
866 collections, promote research and education. *BioScience*, 70(1):23–30, 2020.
- 867 A Leuchtmann. Systematics, distribution, and host specificity of grass endophytes. *Natural toxins*,  
868 1(3):150–162, 1992.

- 869 A Leuchtmann, C W Bacon, C L Schardl, J F White Jr, and M Tadych. Nomenclatural realignment  
870 of *Neotyphodium* species with genus *Epichloë*. *Mycologia*, 106(2):202–215, 2014.
- 871 F Lindgren, H Rue, and J Lindström. An explicit link between gaussian fields and gaussian markov  
872 random fields: the stochastic partial differential equation approach. *Journal of the Royal Statis-*  
873 *tical Society: Series B (Statistical Methodology)*, 73(4):423–498, 2011.
- 874 C Liu, P M Berry, T P Dawson, and R G Pearson. Selecting thresholds of occurrence in the  
875 prediction of species distributions. *Ecography*, 28(3):385–393, 2005.
- 876 D D Mc Cargo, L J Iannone, M V Vignale, C L Schardl, and M S Rossi. Species diversity of  
877 *Epichloë* symbiotic with two grasses from southern Argentinean Patagonia. *Mycologia*, 106(2):  
878 339–352, 2014.
- 879 M McFall-Ngai, M G Hadfield, TCG Bosch, H V Carey, T Domazet-Lošo, A E Douglas, N Dubilier,  
880 G Eberl, T Fukami, S F Gilbert, et al. Animals in a bacterial world, a new imperative for the  
881 life sciences. *Proceedings of the National Academy of Sciences*, 110(9):3229–3236, 2013.
- 882 T D Meehan, N L Michel, and H Rue. Spatial modeling of Audubon Christmas Bird Counts reveals  
883 fine-scale patterns and drivers of relative abundance trends. *Ecosphere*, 10(4):e02707, 2019.
- 884 E K Meineke and B H Daru. Bias assessments to expand research harnessing biological collections.  
885 *Trends in Ecology & Evolution*, 36(12):1071–1082, 2021.
- 886 E K Meineke, C C Davis, and T J Davies. The unrealized potential of herbaria for global change  
887 biology. *Ecological Monographs*, 88(4):505–525, 2018.
- 888 E K Meineke, A T Classen, N J Sanders, and T J Davies. Herbarium specimens reveal increasing  
889 herbivory over the past century. *Journal of Ecology*, 107(1):105–117, 2019.
- 890 A R Meyer, M Valentin, L Liulevicius, T R McDonald, M P Nelsen, J Pengra, R J Smith, and  
891 D Stanton. Climate warming causes photobiont degradation and c starvation in a boreal climate  
892 sentinel lichen. *American Journal of Botany*, 2022.

- 893 D AW Miller, K Pacifici, J S Sanderlin, and B J Reich. The recent past and promising future for  
894 data integration methods to estimate species' distributions. *Methods in Ecology and Evolution*,  
895 10(1):22–37, 2019.
- 896 D S Park, I Breckheimer, A C Williams, E Law, A M Ellison, and C C Davis. Herbarium specimens  
897 reveal substantial and unexpected variation in phenological sensitivity across the eastern United  
898 States. *Philosophical Transactions of the Royal Society B*, 374(1763):20170394, 2019.
- 899 B J Parker, J Hrček, AHC McLean, and H C J Godfray. Genotype specificity among hosts,  
900 pathogens, and beneficial microbes influences the strength of symbiont-mediated protection. *Evo-  
901 lution*, 71(5):1222–1231, 2017.
- 902 M Parniske. Arbuscular mycorrhiza: The mother of plant root endosymbioses. *Nature Reviews  
903 Microbiology*, 6(10):763–775, 2008.
- 904 A Pauw and J A Hawkins. Reconstruction of historical pollination rates reveals linked declines of  
905 pollinators and plants. *Oikos*, 120(3):344–349, 2011.
- 906 S Piao, Q Liu, A Chen, I A Janssens, Y Fu, J Dai, L Liu, X Lian, M Shen, and X Zhu. Plant  
907 phenology and global climate change: Current progresses and challenges. *Global Change Biology*,  
908 25(6):1922–1940, 2019.
- 909 T Poisot, G Bergeron, K Cazelles, T Dallas, D Gravel, A MacDonald, B Mercier, C Violet, and  
910 S Vissault. Global knowledge gaps in species interaction networks data. *Journal of Biogeography*,  
911 48(7):1552–1563, 2021.
- 912 N E Rafferty, P J CaraDonna, and J L Bronstein. Phenological shifts and the fate of mutualisms.  
913 *Oikos*, 124(1):14–21, 2015.
- 914 Emma Chollet Ramampiandra, Andreas Scheidegger, Jonas Wydler, and Nele Schuwirth. A com-  
915 parison of machine learning and statistical species distribution models: Quantifying overfitting  
916 supports model interpretation. *Ecological Modelling*, 481:110353, 2023.

- 917 C J Raxworthy and B T Smith. Mining museums for historical DNA: Advances and challenges in  
918 museomics. *Trends in Ecology & Evolution*, 36(11):1049–1060, 2021.
- 919 F Renoz, I Pons, and T Hance. Evolutionary responses of mutualistic insect–bacterial symbioses in  
920 a world of fluctuating temperatures. *Current Opinion in Insect Science*, 35:20–26, 2019.
- 921 Jean B Ristaino. The importance of mycological and plant herbaria in tracking plant killers. *Fron-  
922 tiers in Ecology and Evolution*, 7:521, 2020.
- 923 Jean B Ristaino, Carol T Groves, and Gregory R Parra. Pcr amplification of the irish potato famine  
924 pathogen from historic specimens. *Nature*, 411(6838):695–697, 2001.
- 925 Jean Beagle Ristaino. Tracking historic migrations of the irish potato famine pathogen, phytoph-  
926 thora infestans. *Microbes and infection*, 4(13):1369–1377, 2002.
- 927 E L Roberts and A Ferraro. Rhizosphere microbiome selection by *Epichloë* endophytes of *Festuca*  
928 *arundinacea*. *Plant and Soil*, 396:229–239, 2015.
- 929 RJ Rodriguez, JF White Jr, Anne E Arnold, and a RS and Redman. Fungal endophytes: diversity  
930 and functional roles. *New Phytologist*, 182(2):314–330, 2009.
- 931 G Rolshausen, F Dal Grande, A D Sadowska-Deś, J Otte, and I Schmitt. Quantifying the climatic  
932 niche of symbiont partners in a lichen symbiosis indicates mutualist-mediated niche expansions.  
933 *Ecography*, 41(8):1380–1392, 2018.
- 934 J A Rudgers, M E Afkhami, M A Rúa, A J Davitt, S Hammer, and V M Huguet. A fungus among  
935 us: broad patterns of endophyte distribution in the grasses. *Ecology*, 90(6):1531–1539, 2009.
- 936 J A Rudgers, M E Afkhami, L Bell-Dereske, Y A Chung, K M Crawford, S N Kivlin, M A Mann,  
937 and M A Nuñez. Climate disruption of plant-microbe interactions. *Annual review of ecology,  
938 evolution, and systematics*, 51(1):561–586, 2020.
- 939 Jennifer A Rudgers and Angela L Swafford. Benefits of a fungal endophyte in *Elymus virginicus*  
940 decline under drought stress. *Basic and Applied Ecology*, 10(1):43–51, 2009.

- 941 H Rue, S Martino, and N Chopin. Approximate bayesian inference for latent gaussian models by  
942 using integrated nested laplace approximations. *Journal of the royal statistical society: Series b*  
943 (*statistical methodology*), 71(2):319–392, 2009.
- 944 R F Sage. Global change biology: a primer. *Global Change Biology*, 26(1):3–30, 2020.
- 945 K Saikkonen, P E Gundel, and M Helander. Chemical ecology mediated by fungal endophytes in  
946 grasses. *Journal of chemical ecology*, 39:962–968, 2013.
- 947 C L Schardl, C A Young, J R Faulkner, S Florea, and J Pan. Chemotypic diversity of *Epichloae*,  
948 fungal symbionts of grasses. *Fungal Ecology*, 5(3):331–344, 2012.
- 949 Ryan J Schmidt, Kristen E Saban, Lena Struwe, and Charles C Davis. The collector practices that  
950 shape spatial, temporal, and taxonomic bias in herbaria. *New Phytologist*.
- 951 María Semmartin, Marina Omacini, Pedro E Gundel, and Ignacio M Hernández-Agramonte. Broad-  
952 scale variation of fungal-endophyte incidence in temperate grasses. *Journal of Ecology*, 103(1):  
953 184–190, 2015.
- 954 S I Seneviratne, X Zhang, M Adnan, W Badi, C Dereczynski, A D Luca, S Ghosh, I Iskandar,  
955 J Kossin, S Lewis, et al. Weather and climate extreme events in a changing climate. 2021.
- 956 D Simpson, H Rue, A Riebler, T G Martins, and S H Sørbye. Penalising model component com-  
957 plexity: A principled, practical approach to constructing priors. 2017.
- 958 Brajesh K Singh, Manuel Delgado-Baquerizo, Eleonora Egidi, Emilio Guirado, Jan E Leach, Hong-  
959 wei Liu, and Pankaj Trivedi. Climate change impacts on plant pathogens, food security and paths  
960 forward. *Nature Reviews Microbiology*, 21(10):640–656, 2023.
- 961 Michelle E Sneck, Jennifer A Rudgers, Carolyn A Young, and Tom EX Miller. Variation in the  
962 prevalence and transmission of heritable symbionts across host populations in heterogeneous en-  
963 vironments. *Microbial Ecology*, 74:640–653, 2017.

- 964 Pamela S Soltis. Digitization of herbaria enables novel research. *American journal of botany*, 104  
965 (9):1281–1284, 2017.
- 966 T F Stocker, D Qin, G-K Plattner, L V Alexander, S K Allen, N L Bindoff, F-M Bréon, J A Church,  
967 U Cubasch, S Emori, et al. Technical summary. In *Climate Change 2013: The Physical Science  
968 Basis. Contribution of Working Group I to the Fifth Assessment Report of the Intergovernmental  
969 Panel on Climate Change*, pages 33–115. Cambridge University Press, 2013.
- 970 P A Stott, N P Gillett, G C Hegerl, D J Karoly, D A Stone, X Zhang, and F Zwiers. Detection and  
971 attribution of climate change: A regional perspective. *Wiley Interdisciplinary Reviews: Climate  
972 Change*, 1(2):192–211, 2010.
- 973 S Sully, DE Burkepile, MK Donovan, G Hodgson, and R Van Woesik. A global analysis of coral  
974 bleaching over the past two decades. *Nature communications*, 10(1):1–5, 2019.
- 975 E Toby Kiers, T M Palmer, A R Ives, J F Bruno, and J L Bronstein. Mutualisms in a changing  
976 world: an evolutionary perspective. *Ecology Letters*, 13(12):1459–1474, 2010.
- 977 A T Tredennick, G Hooker, S P Ellner, and P B Adler. A practical guide to selecting models for  
978 exploration, inference, and prediction in ecology. *Ecology*, 102(6):e03336, 2021.
- 979 A D Treindl, J Stapley, and A Leuchtmann. Genetic diversity and population structure of *Epichloë*  
980 fungal pathogens of plants in natural ecosystems. *Frontiers in Ecology and Evolution*, 11:1129867,  
981 2023.
- 982 K E Trenberth, J T Fasullo, and T G Shepherd. Attribution of climate extreme events. *Nature  
983 Climate Change*, 5(8):725–730, 2015.
- 984 A M Truitt, M Kapun, R Kaur, and W J Miller. Wolbachia modifies thermal preference in drosophila  
985 melanogaster. *Environmental microbiology*, 21(9):3259–3268, 2019.
- 986 Shripad D. Tuljapurkar. Population dynamics in variable environments. III. Evolutionary dynamics  
987 of r-selection. *Theoretical Population Biology*, 21(1):141–165, February 1982. ISSN 0040-5809.

- 988 doi: 10.1016/0040-5809(82)90010-7. URL <http://www.sciencedirect.com/science/article/pii/0040580982900107>.
- 990 A Urdangarin, T Goicoa, and M D Ugarte. Evaluating recent methods to overcome spatial con-  
991 founding. *Revista Matemática Complutense*, 36(2):333–360, 2023.
- 992 V Vikuk, C A Young, S T Lee, P Nagabhyru, M Krischke, M J Mueller, and J Krauss. Infection  
993 rates and alkaloid patterns of different grass species with systemic *Epichloë* endophytes. *Applied*  
994 *and Environmental Microbiology*, 85(17):e00465–19, 2019.
- 995 M von Cräutlein, M Helander, H Korpelainen, P H Leinonen, B R Vázquez de Aldana, C A Young,  
996 I Zabalzogea, and K Saikkonen. Genetic diversity of the symbiotic fungus *Epichloë festucae*  
997 in naturally occurring host grass populations. *Frontiers in Microbiology*, 12:756991, 2021.
- 998 Z Wang, C Li, and J White. Effects of *Epichloë* endophyte infection on growth, physiological  
999 properties and seed germination of wild barley under saline conditions. *Journal of Agronomy and*  
1000 *Crop Science*, 206(1):43–51, 2020.
- 1001 Eric J Ward, Eli E Holmes, James T Thorson, and Ben Collen. Complexity is costly: a meta-  
1002 analysis of parametric and non-parametric methods for short-term population forecasting. *Oikos*,  
1003 123(6):652–661, 2014.
- 1004 R J Warren and M A Bradford. Mutualism fails when climate response differs between interacting  
1005 species. *Global Change Biology*, 20(2):466–474, 2014.
- 1006 N S Webster, R E Cobb, and A P Negri. Temperature thresholds for bacterial symbiosis with a  
1007 sponge. *The ISME journal*, 2(8):830–842, 2008.
- 1008 J F White and G T Cole. Endophyte-host associations in forage grasses. i. Distribution of fungal  
1009 endophytes in some species of *Lolium* and *Festuca*. *Mycologia*, 77(2):323–327, 1985.
- 1010 F M Willems, JF Scheepens, and O Bossdorf. Forest wildflowers bloom earlier as europe warms:  
1011 Lessons from herbaria and spatial modelling. *New Phytologist*, 235(1):52–65, 2022.

- 1012 C G Willis, E R Ellwood, R B Primack, C C Davis, K D Pearson, A S Gallinat, J M Yost, G Nelson,  
1013 S J Mazer, N L Rossington, et al. Old plants, new tricks: Phenological research using herbarium  
1014 specimens. *Trends in Ecology & Evolution*, 32(7):531–546, 2017.
- 1015 C Xia, N Li, Y Zhang, C Li, X Zhang, and Z Nan. Role of *Epichloë* endophytes in defense responses  
1016 of cool-season grasses to pathogens: A review. *Plant Disease*, 102(11):2061–2073, 2018.
- 1017 K Yoshida, E Sasaki, and S Kamoun. Computational analyses of ancient pathogen DNA from  
1018 herbarium samples: Challenges and prospects. *Frontiers in Plant Science*, 6:771, 2015.
- 1019 Kentaro Yoshida, Verena J Schuenemann, Liliana M Cano, Marina Pais, Bagdevi Mishra, Rahul  
1020 Sharma, Chirsta Lanz, Frank N Martin, Sophien Kamoun, Johannes Krause, et al. The rise and  
1021 fall of the *Phytophthora infestans* lineage that triggered the irish potato famine. *elife*, 2:e00731,  
1022 2013.

1023

## Appendix A

1024

1025     *Appendix to "Increasing Prevalence of plant-fungal symbiosis across two  
1026                         centuries of environmental change"*

1027     **Authors:**

1028     Joshua C. Fowler<sup>1,2\*</sup>

1029     Jacob Moutouama<sup>1</sup>

1030     Tom E. X. Miller<sup>1</sup>

1031

1032     1. Rice University, Department of BioSciences, Houston, Texas 77006

1033     2. University of Miami, Department of Biology, Miami, Florida

1034     \* Corresponding author; e-mail: jcf221@miami.edu.

1035     **Contents:**

1036     Appendix A includes: Figure A1 - Figure A15, Table A1, and Supporting Methods).

1037

## Supplemental Figures

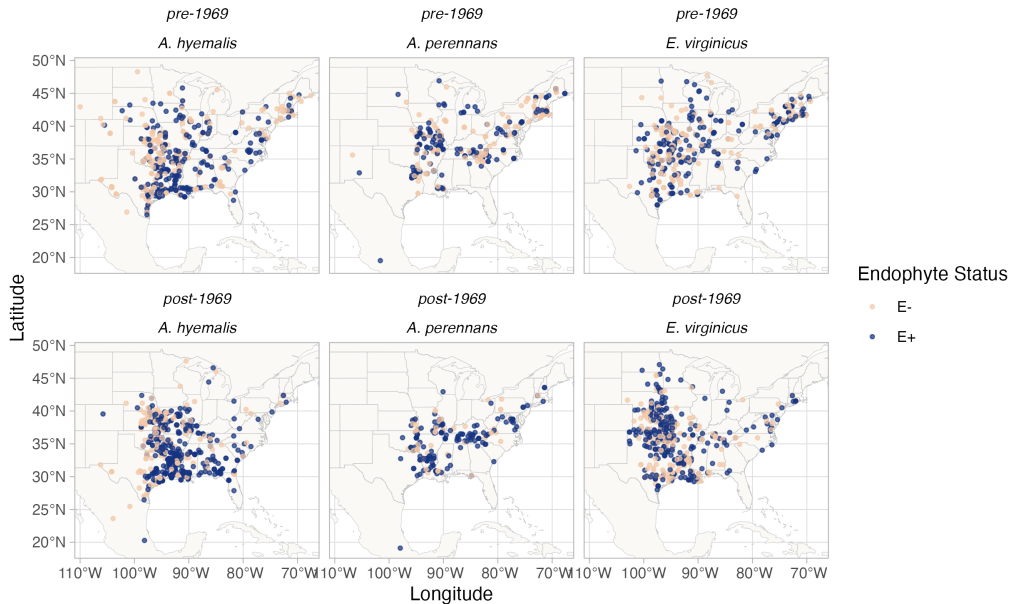


**Figure A1: Endophyte presence/absence in specimens of each host species.** Points show collection locations colored according to whether the specimen contained endophytes ( E+; blue points) or did not contain endophytes (E-, tan points). To visualize temporal change, the data are faceted before and after the median year of collection. Map lines delineate study areas and do not necessarily depict accepted national boundaries.

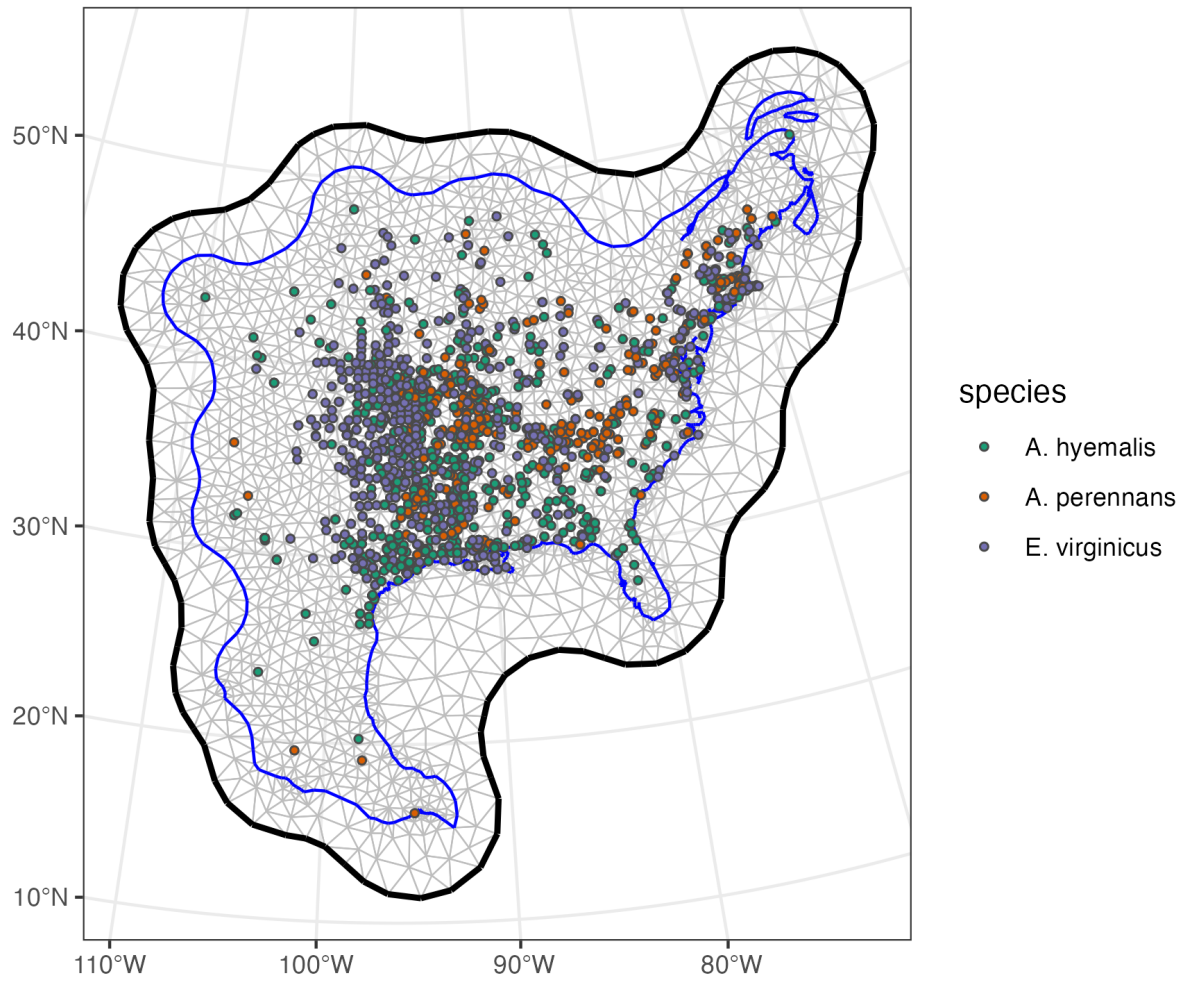


Figure A2: **Triangulation mesh used to estimate spatial dependence between data points.**

Grey lines indicate edges of triangles used to define distances between observations. Colored points indicate locations of sampled herbarium specimens for each host species, and the blue line shows the convex hull and coastline used to define the edge of the mesh around the data points. The thick black line shows the convex hull defining a buffer space around the edge of the mesh to reduce the influence of edge effects on model estimates.

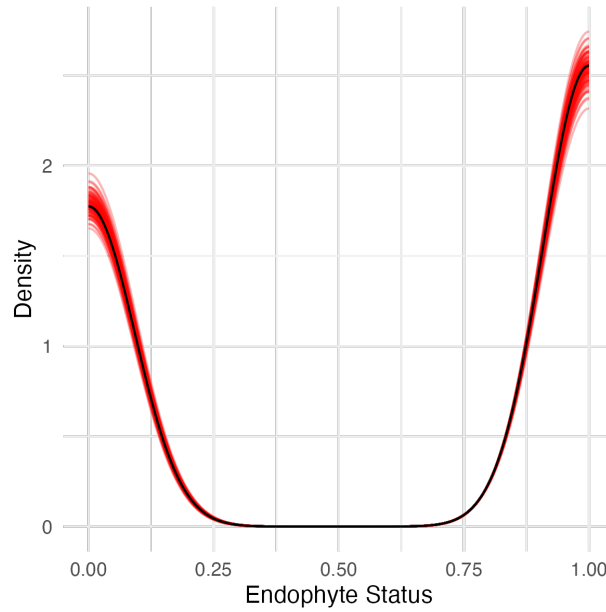
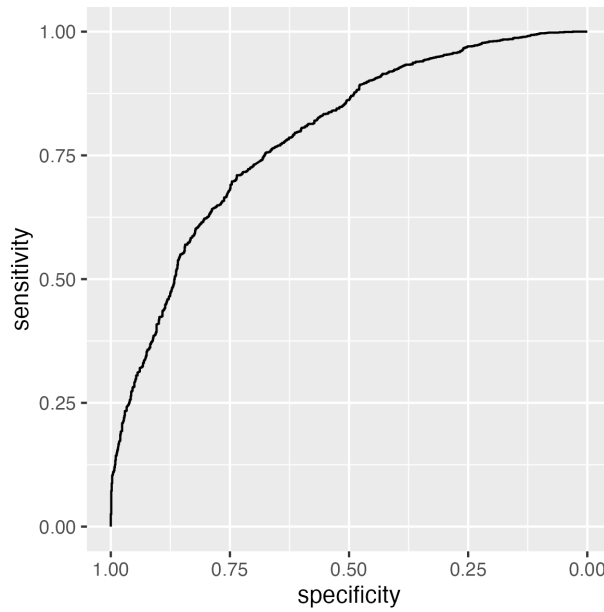
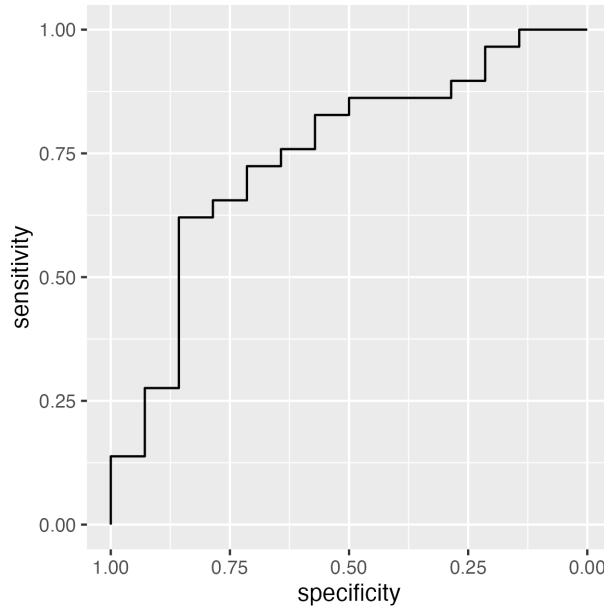


Figure A3: **Graphical posterior predictive check of the endophyte prevalence model fit.**

Consistency between observed data and predicted values indicate that the fitted model accurately describes the data. Graph shows density curves for the observed data (black) along with 100 predicted datasets (red).



**Figure A4: ROC plot showing performance of the endophyte prevalence model in classifying observations according to endophyte status within the in-sample training data from herbarium collections.** The curves show adequate model performance for observed data. The AUC value is 0.79.



**Figure A5: ROC plot showing performance of the endophyte prevalence model in classifying observations according to endophyte status within the out-of-sample test data from contemporary surveys.** The curves show adequate model performance for test data. The AUC value is 0.77.

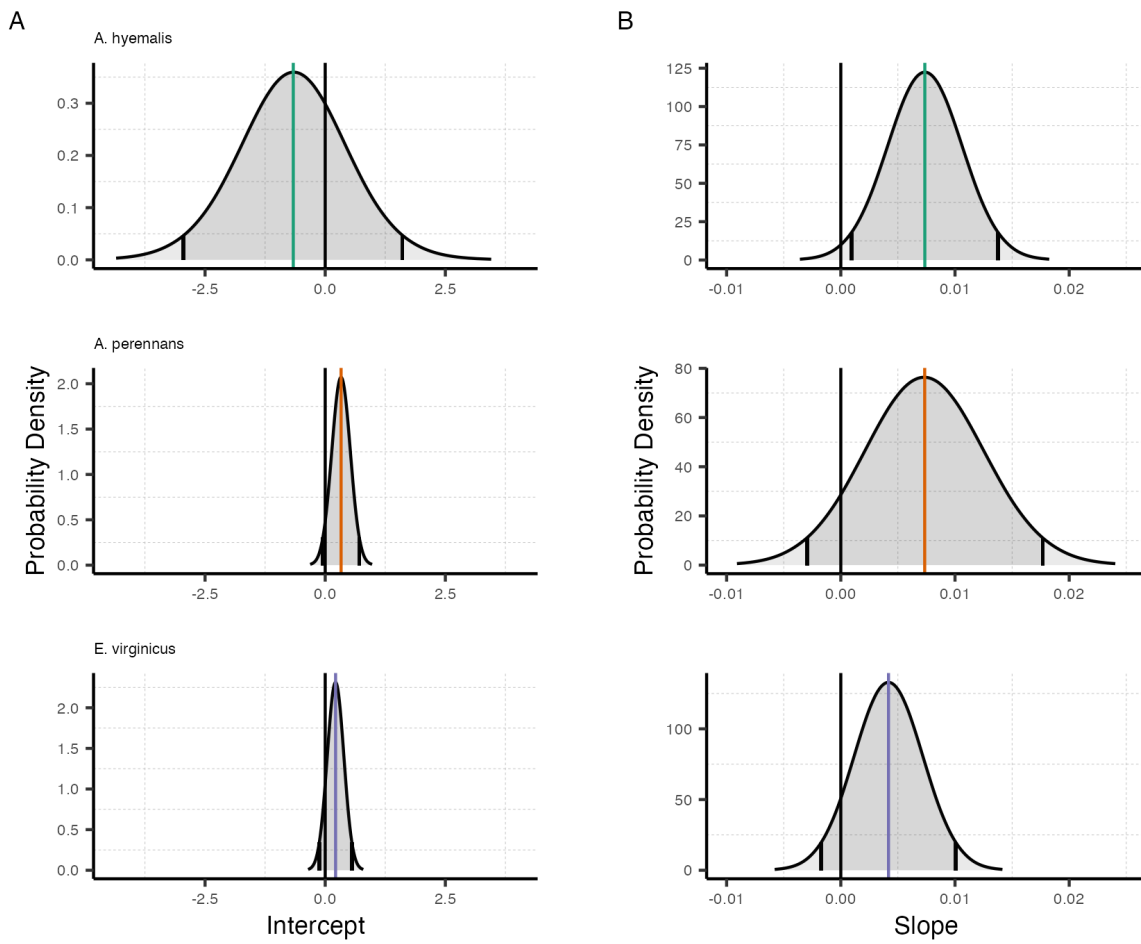


**Figure A6: Posterior estimates of parameters describing global intercept and temporal trends from the endophyte prevalence model.** Density curves show the probability density along with mean (colored line) and 95% CI (black lines) for the (A) intercept and (B) slope terms,  $A$  and  $T$  respectively from Eqn. 1. Colors represent each host species

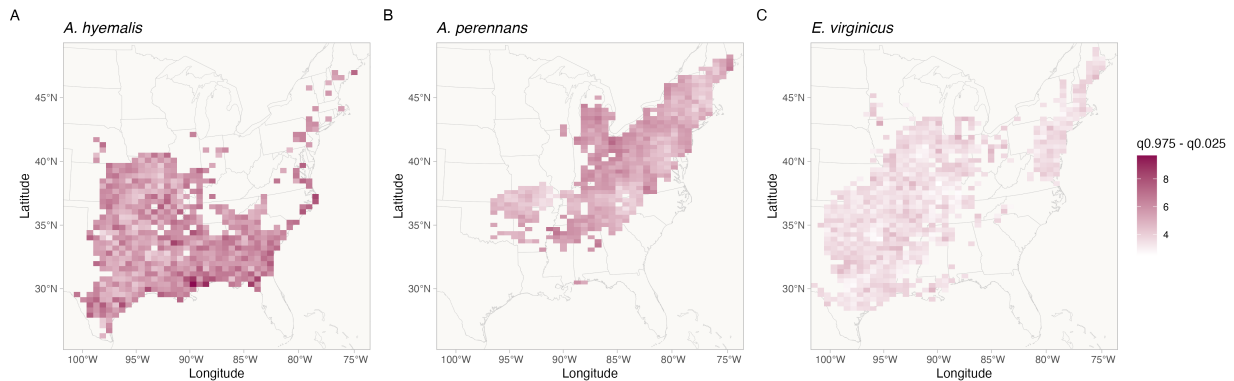


**Figure A7: Credible interval width of temporal trends in endophyte prevalence across the distribution of each host species estimated from the endophyte prevalence model.**  
 Shading represents the range of the 95% posterior credible interval given in units of *% change in prevalence/year* for spatially varying slopes,  $\tau$  from Eqn. 1. Map lines delineate study areas and do not necessarily depict accepted national boundaries.

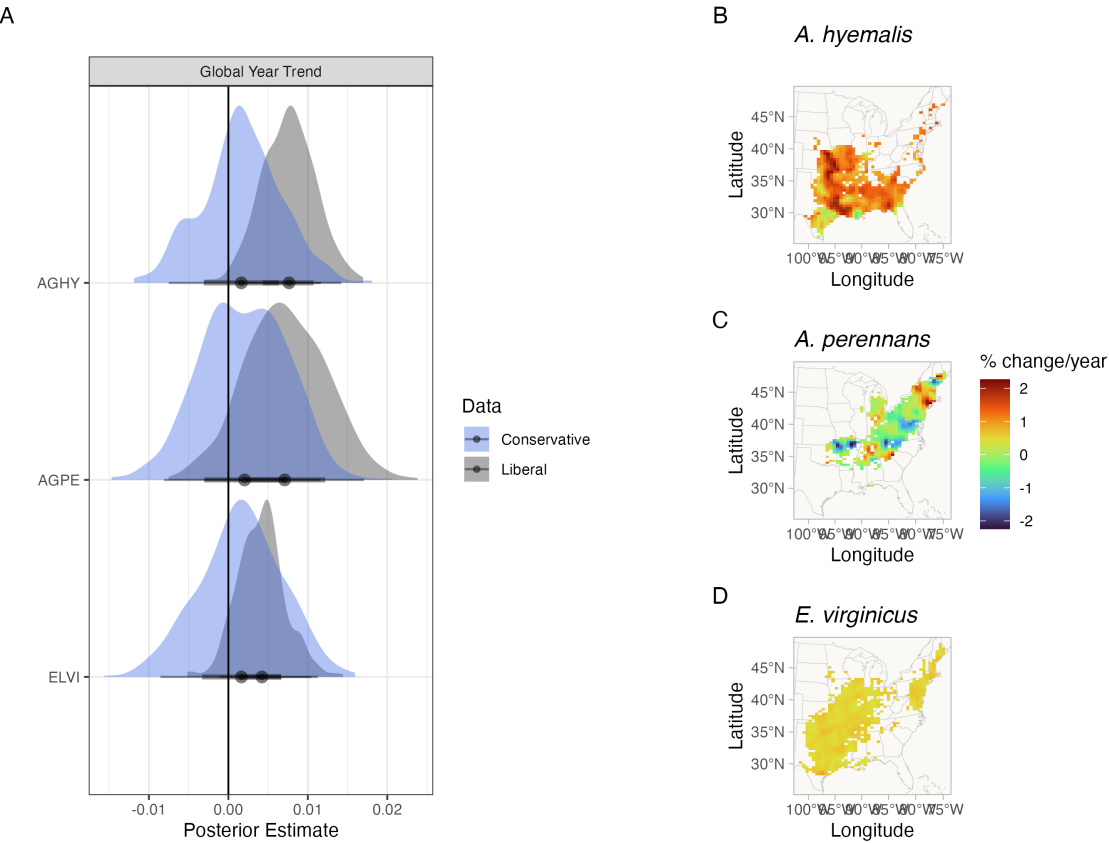


**Figure A8: Comparison of endophyte prevalence model estimates fit to data with liberal versus conservative endophyte scores.** Liberal and conservative scores document uncertainty in the endophyte identification process. Each specimen was given both a liberal and conservative scores. In cases of uncertain identification, the liberal status assumed a potential endophyte identification was more likely to be endophyte-positive while the conservative status assumed that the potential endophyte identification was less likely to be endophyte-positive. (A) Posterior estimates of global temporal trend ( $T$  from Eqn. 1) for the endophyte prevalence model fit to liberal scores (grey) and to conservative scores (blue). Maps show the spatially varying temporal trend estimates ( $\tau$  from Eqn. 1) from the endophyte prevalence model fit to conservative scores for (B) *A. hyemalis*, (C) *A. perennans*, and (D) *E. virginicus*. Note that the color scale differs between this visualization and Fig. 3 that shows estimates fit using liberal endophyte scores.

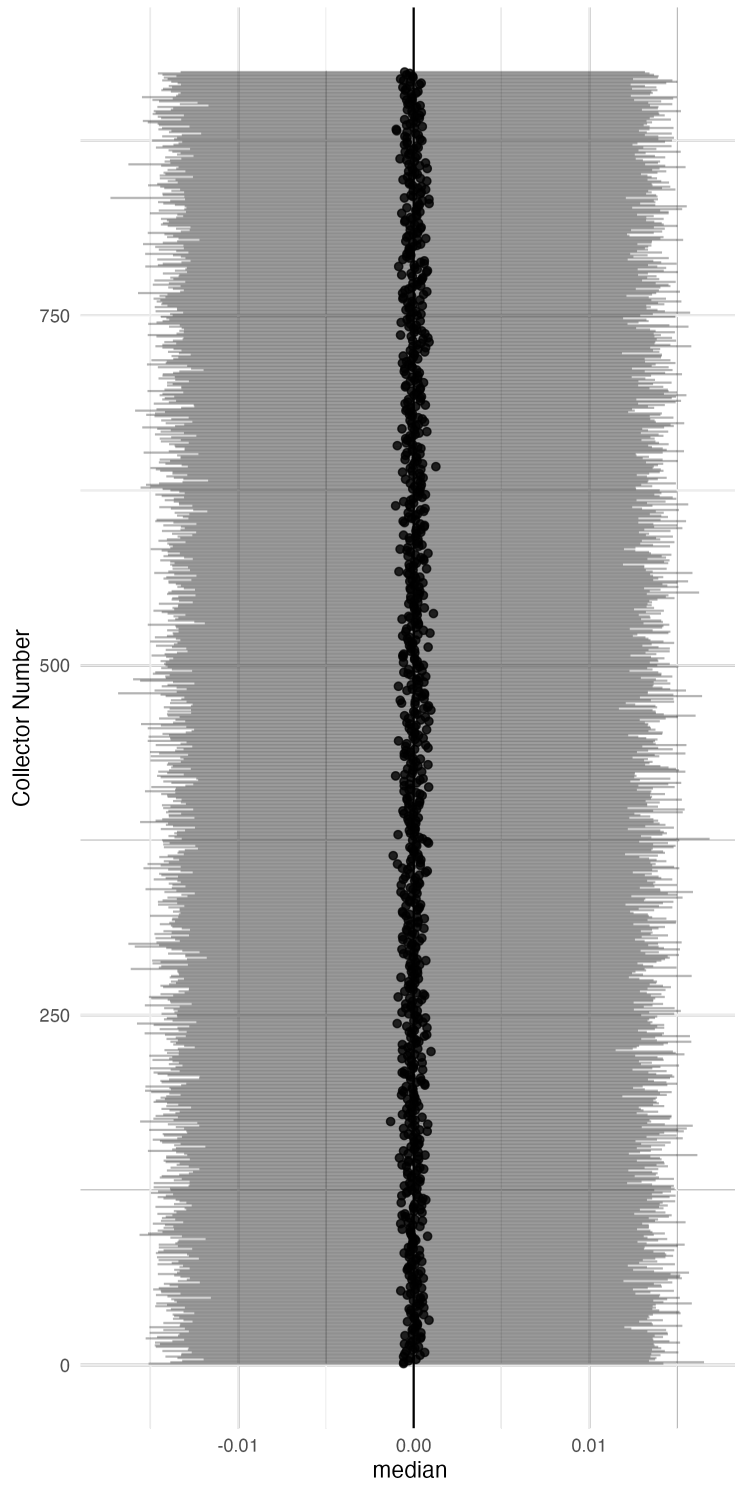


Figure A9: **Posterior estimates of collector random effects from endophyte prevalence model.** Collector random effects are denoted  $\chi$  in Eqn. 1 and represent variance associated with researchers who collected historic herbarium specimens. Points show posterior median along with 95% CI for each of 924 individual collectors.

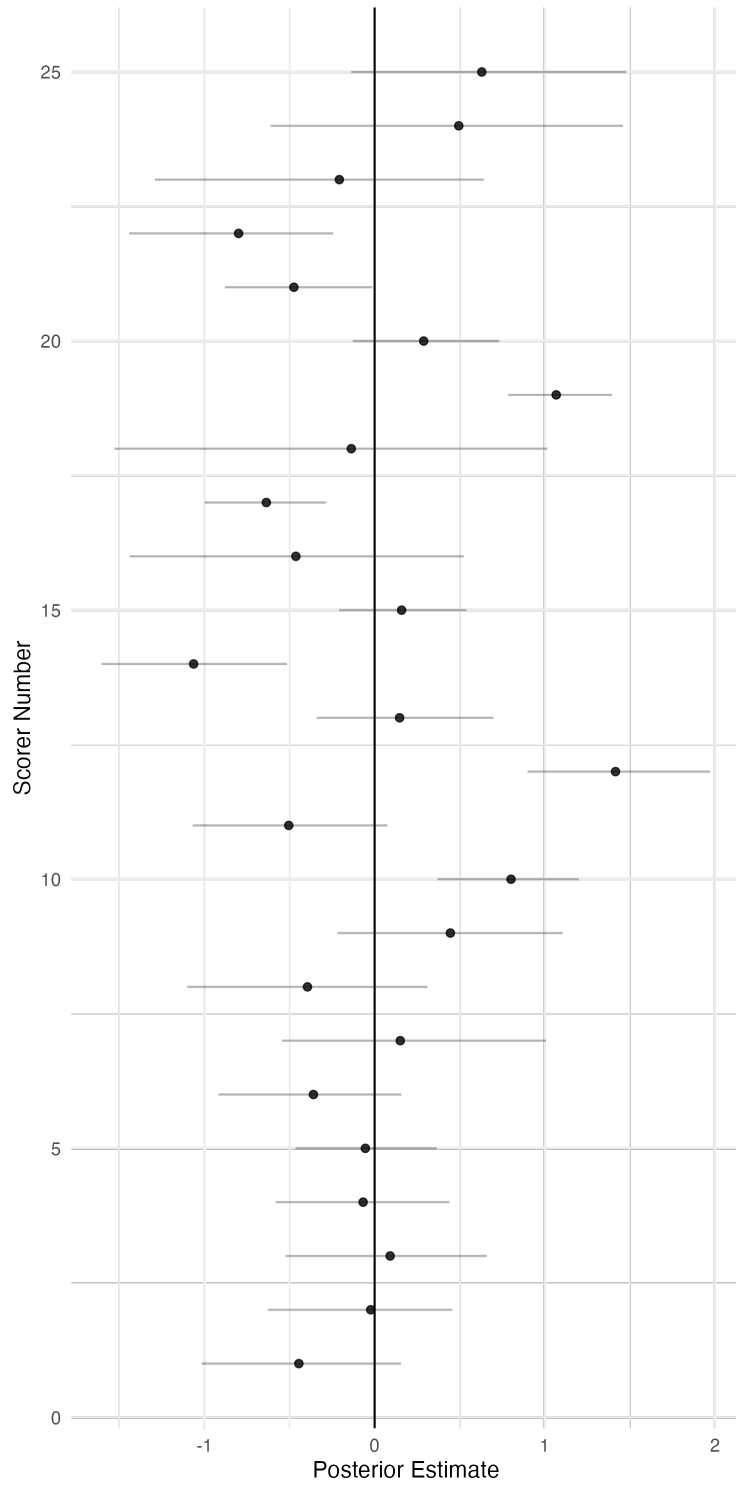
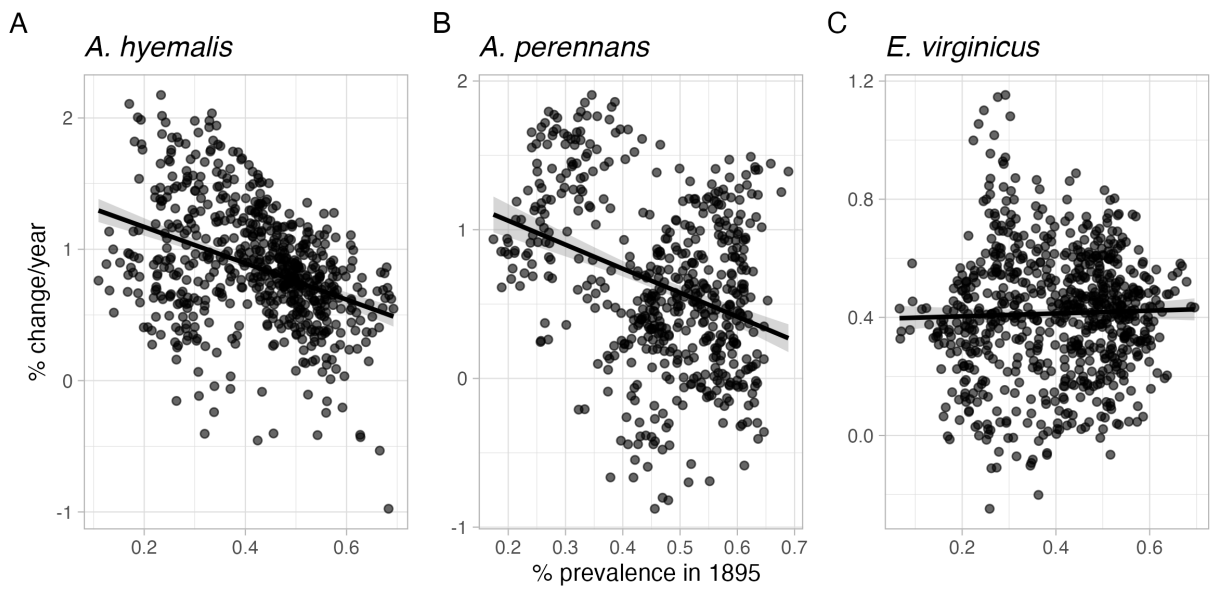
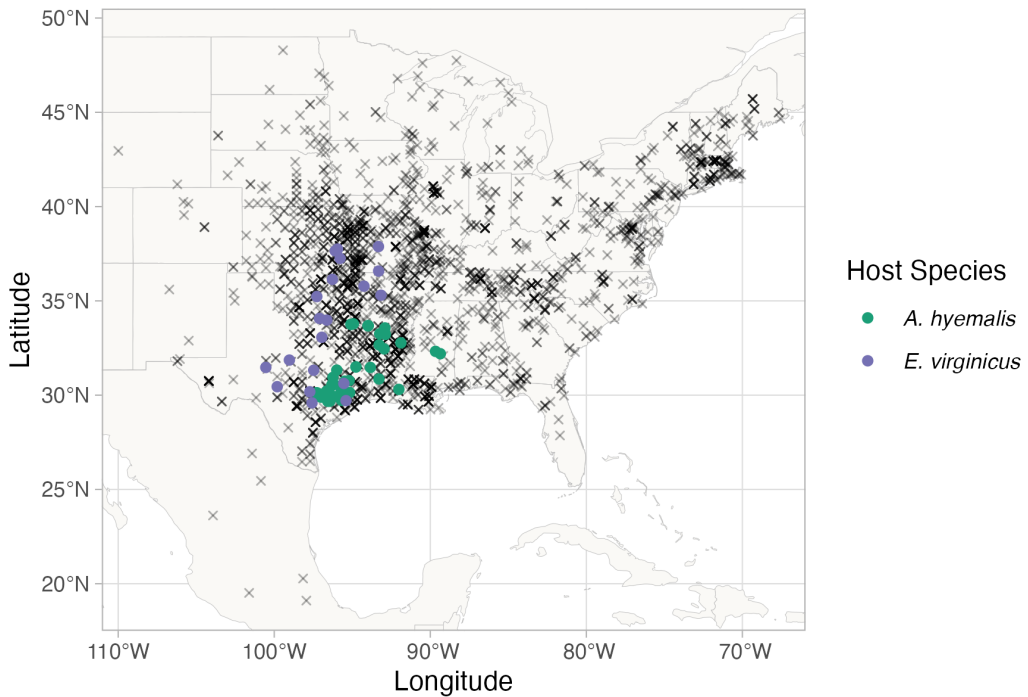


Figure A10: **Posterior estimates of scorer random effects from endophyte prevalence model.** Scorer random effects are denoted  $\omega$  in Eqn. 1 and represent variance associated with researchers who identified *Epichloë* endophytes within herbarium specimen tissue samples. Points show posterior median along with 95% CI for each of 25 individual scorers.



**Figure A11: Relationship between initial prevalence and temporal trends in prevalence estimated from the endophyte prevalence model.** Points show predicted posterior mean temporal trend for each species at pixels across each host distribution ((A) *A. hyemalis*, (B) *A. perennans*, and (C) *E. virginicus*). along with a linear regression and shaded ribbon showing 95% confidence interval.



**Figure A12: Locations of contemporary surveys of endophytes used as "test" data to evaluate predictive ability of the endophyte prevalence model.** Points are locations of host populations surveyed between 2013 and 2019 for endophytes, colored by species (*A. hyemalis*: green, *E. virginicus*: purple). Black crosses show the historical herbarium collection locations used as "training" data for the endophyte prevalence model.

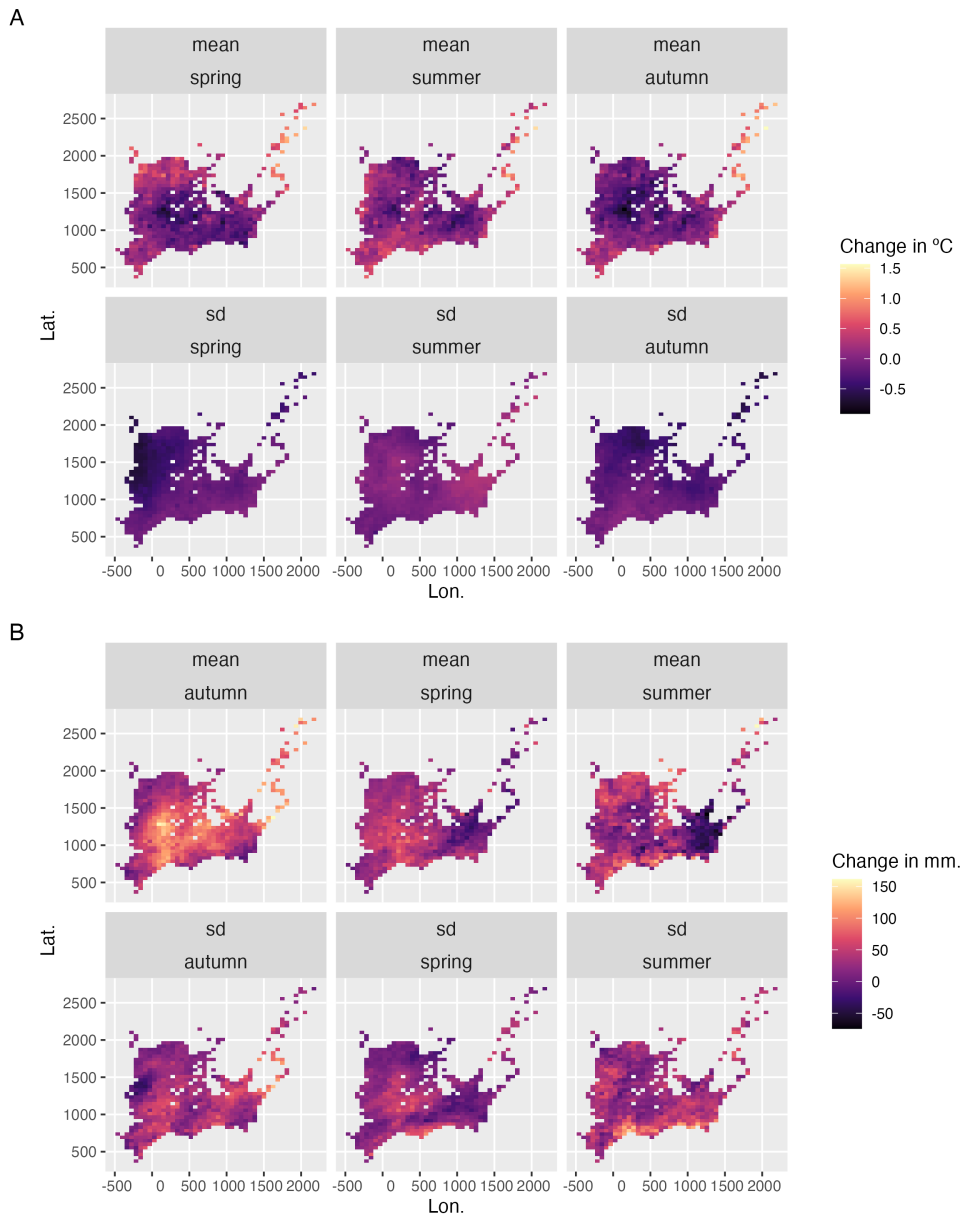
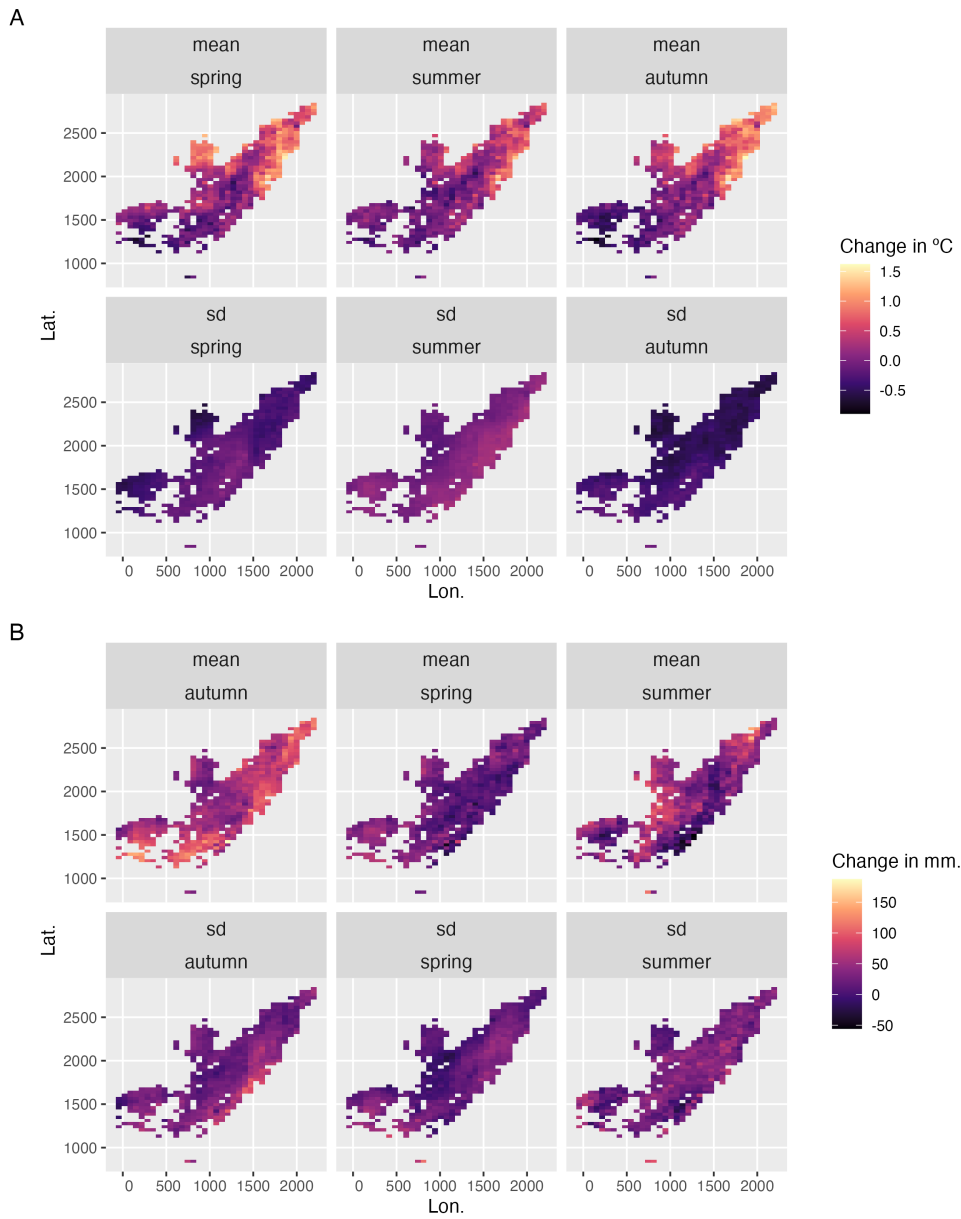


Figure A13: **Change in seasonal climate variables between the periods 1895-1925 and 1990-2020 across the distribution of *A. hyemalis*.** Color represents change in (A) seasonal temperature ( $^{\circ}\text{C}$ ) and (B) seasonal precipitation (mm.). Maps show pixels covering the modeled distribution of *A. hyemalis* used in *post hoc* climate regression analysis.



**Figure A14: Change in seasonal climate variables between the periods 1895-1925 and 1990-2020 across the distribution of *A. perennans*.** Color represents change in (A) seasonal temperature ( $^{\circ}\text{C}$ ) and (B) seasonal precipitation (mm.). Maps show pixels covering the modeled distribution of *A. perennans* used in *post hoc* climate regression analysis.

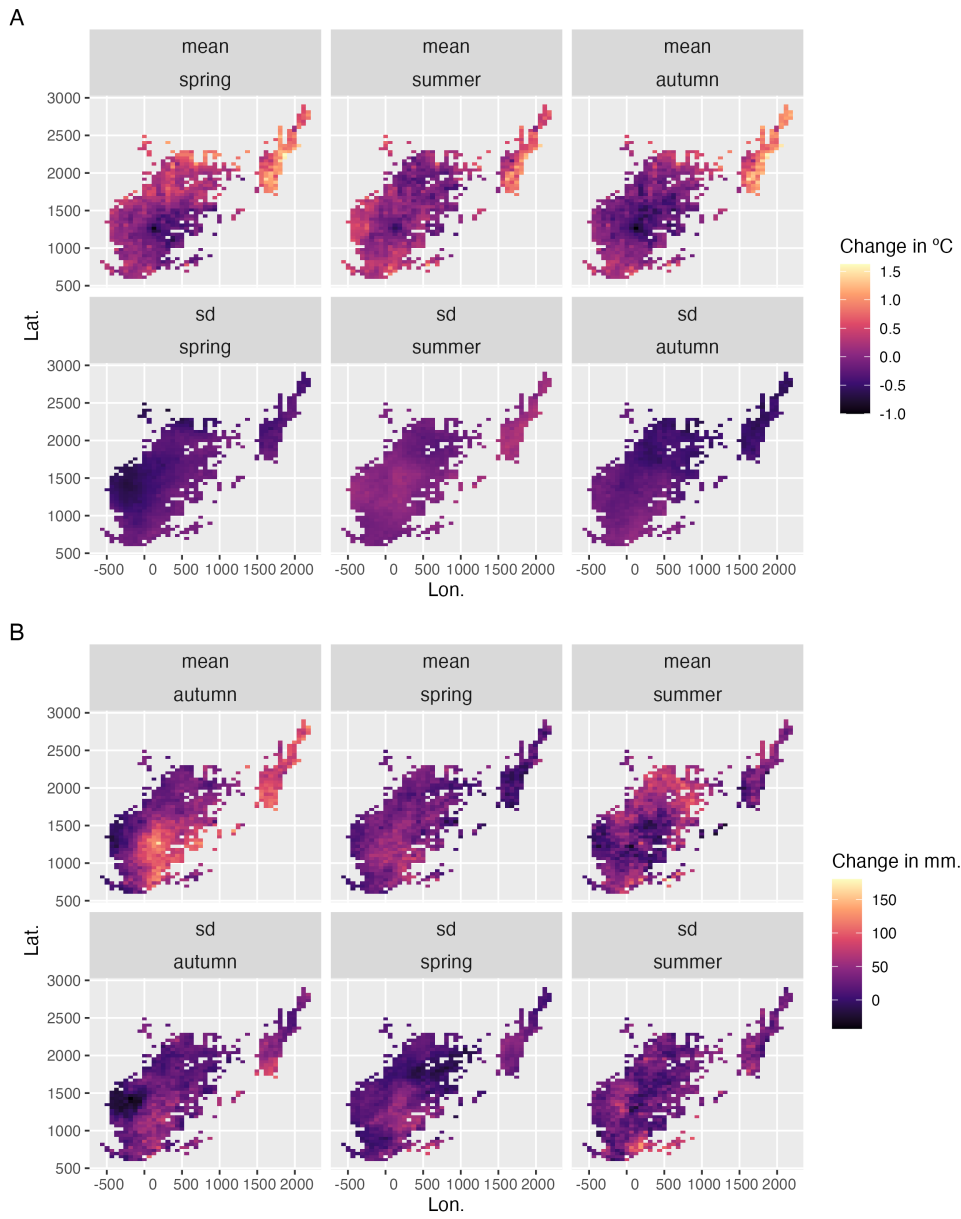


Figure A15: **Change in seasonal climate variables between the periods 1895-1925 and 1990-2020 across the distribution of *E. virginicus*.** Color represents change in (A) seasonal temperature ( $^{\circ}\text{C}$ ) and (B) seasonal precipitation (mm.). Maps show pixels covering the modeled distribution of *E. virginicus* used in *post hoc* climate regression analysis.

Table A1: Summary of herbarium samples across collections (no. of specimens)

| Herbarium Collection                  | <i>A. hyemalis</i> | <i>A. perennans</i> | <i>E. virginicus</i> |
|---------------------------------------|--------------------|---------------------|----------------------|
| Botanical Research Institute of Texas | 350                | 190                 | 198                  |
| Louisiana State University            | 72                 | 38                  | 62                   |
| Mercer Botanic Garden                 | 3                  | 0                   | 6                    |
| Missouri Botanic Garden               | 210                | 205                 | 122                  |
| Texas A&M                             | 100                | 0                   | 72                   |
| University of Kansas                  | 134                | 34                  | 197                  |
| University of Oklahoma                | 85                 | 34                  | 95                   |
| University of Texas & Lundell         | 183                | 91                  | 102                  |
| Oklahoma State University             | 51                 | 10                  | 74                   |

1039

## Supporting Methods

1040

### ODMAP Protocol

1041 [Overview](#)

1042 **Model purpose:** Mapping current distribution of *Epichloë* host species.

1043 **Target species:** *Agrostis hyemalis*, *Agrostis perennans*, and *Elymus virginicus*.

1044 **Study area:** Eastern North America

1045 **Spatial extent:** -125.0208, -66.47917, 24.0625, 49.9375 (xmin, xmax, ymin, ymax).

1046 **Spatial resolution:** 0.04166667, 0.04166667 (x, y).

1047 **Temporal extent:** 1990 to 2020.

1048 **Boundary:** Natural.

1049 [Data](#)

1050 **Observation type:** Occurrence records from Global Biodiversity Information Facility and

1051 herbarium collection across eastern North America. We used 713 occurrences records for *Agrostis*  
1052 *hyemalis*, 656 occurrence records for *Agrostis perennans* and 2338 for *Elymus virginicus*.

1053 **Response data type:** occurrence record, presence-only.

1054 **Coordinate reference system:** WGS84 coordinate reference system (EPSG:4326 code)

1055 **Climatic data:** raster data extracted from PRISM; 30-year normal mean and standard deviation  
1056 of temperature and of precipitation for three four-month seasons within the year (Spring: January,  
1057 February, March, April; Summer: May, June, July, August; Autumn: September, October,  
1058 November, December).

1059 **Model**

1060 **Model assumption:** We assumed that the target species are at equilibrium with their environ-  
1061 ment.

1062 **Algorithms:** Maximum entropy (maxent)

1063 **Workflow:** We described the workflow in the methods section of the manuscript.

1064 **Software:** All statistics were performed using Maxent 3.3.4 and R4.3.1 with packages terra, usdm,  
1065 spThin and dismo.

1066 **Code availability:** Available through this link: <https://github.com/joshuacfowler/EndoHerbarium>

1067 **Data availability:** Data was accessed through open-source R packages *rgbif*. *A. hyemalis*  
1068 (GBIF.Org, 2025a), *A. perennans* (GBIF.Org, 2025b), *E. virginicus* (GBIF.Org, 2025c)

1069 **Assessment**

1070 We used AUC to test model performance.

1071 **Prediction**

1072 We predicted the probability of presence of the host species as a binary maps (presence or absence)

### 1073 *Mesh and Prior Sensitivity Analysis*

1074 To test the influence that the triangulation mesh and choice of priors has on results, we compared  
1075 model results across a range of meshes and priors. We re-ran our model for the mesh used in main  
1076 body of the text (Fig. A2), which we refer to as the "standard mesh", and with a mesh with smaller

1077 minimum vertices (finer mesh). Finer scale meshes increase computation time. For each of these  
1078 meshes, we ran the model with a range of priors defining the spatial range of our spatial random  
1079 effects: 342km (the prior used for presented results), as well as ranges five times smaller (68 km)  
1080 and five times larger (1714 km). We found generally that these choices did not alter the direction  
1081 of model predictions, but did influence the associated uncertainty and magnitude of some effects.

1082 For overall temporal trends, we found that models with differing priors predicted consistently  
1083 positive relationships over time (Fig. A16).

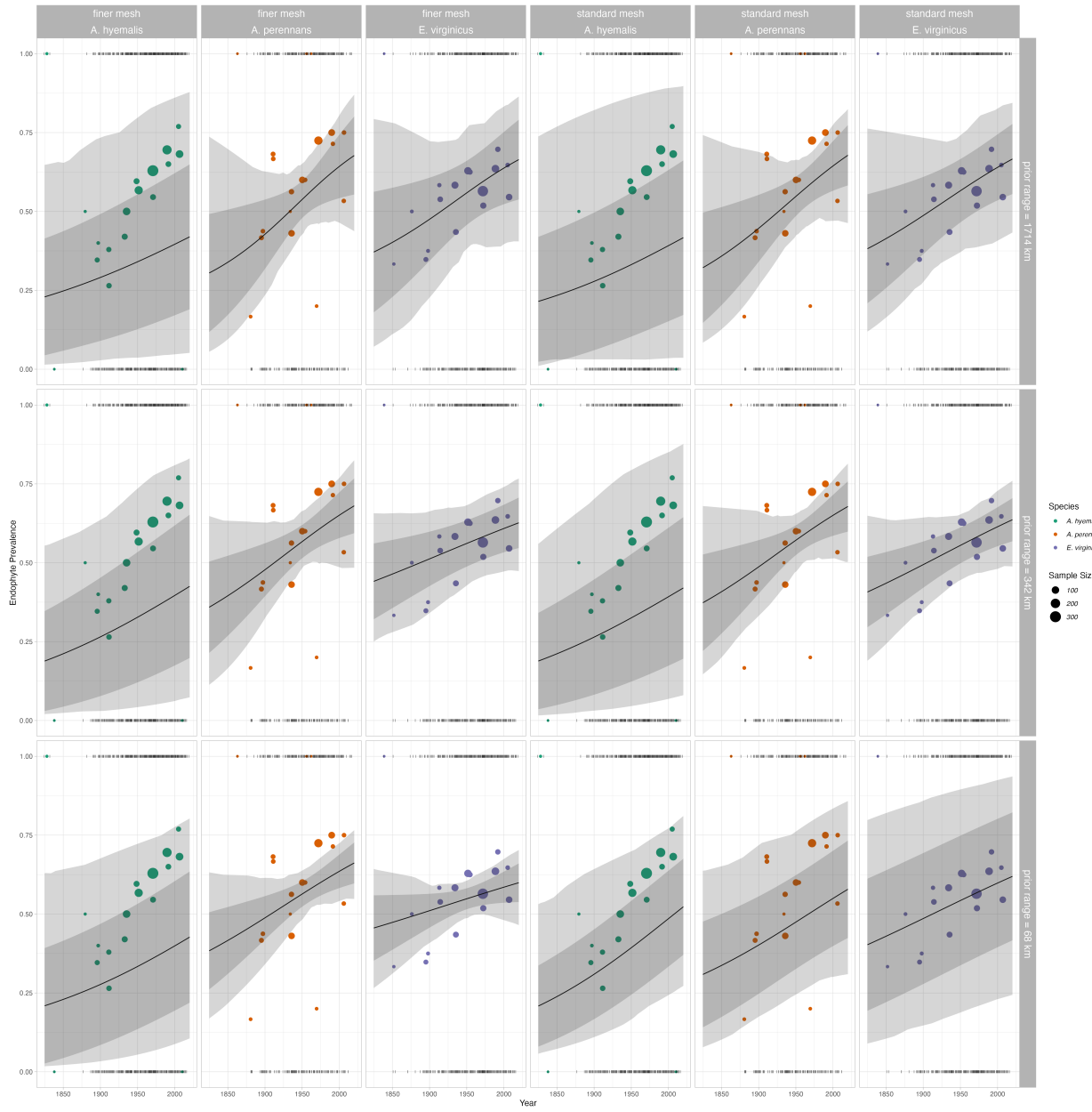


**Figure A16: Overall trend in endophyte prevalence evaluated for endophyte prevalence models with different range priors on spatially structured random effects, and for two different triangulation meshes.** Data used in model fitting is the same across all panels and as in the main text. Note that these plots, as compared to Fig. 2 in main text, show mean trends and do not incorporate variance associated with collector and scorer random effects.

1084 For spatially-varying temporal trends, we found that models with different priors predicted  
1085 consistent spatial patterns in temporal trends, although the range of this prediction varied depending  
1086 on the prior and mesh (Fig. A17 - A18). One noteworthy result of this analysis is that combinations  
1087 of prior choice and mesh can introduce instability in model fitting. This is evident in A17 panel B  
1088 and A18 panel B, where the prior range is smaller than the minimum vertex length of the mesh.  
1089 Model fitting takes an extended time period and the model struggles to identify variation across  
1090 space. Results with a set of prior ranges (Fig. A17 - A and C; Fig. A18 - A and C) result in  
1091 models that estimate trends across space of the same direction and order of magnitude, although  
1092 the "smoothness" of these predictions vary.

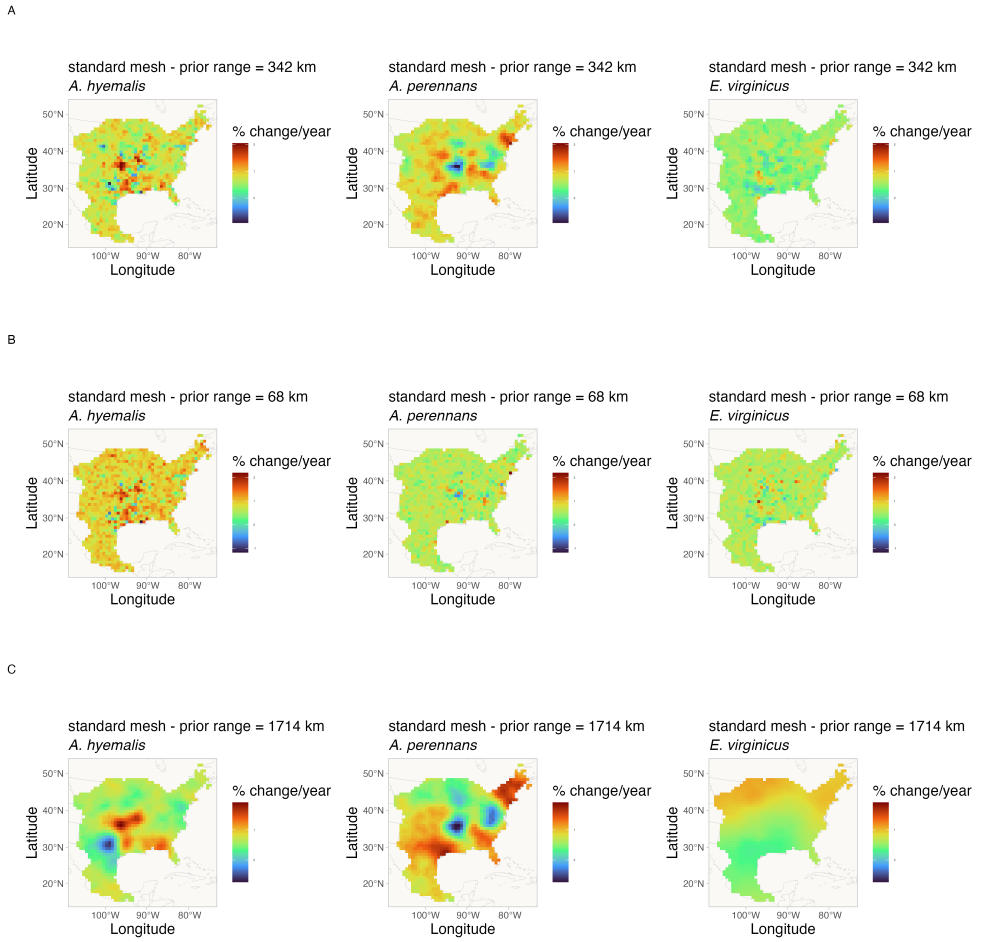
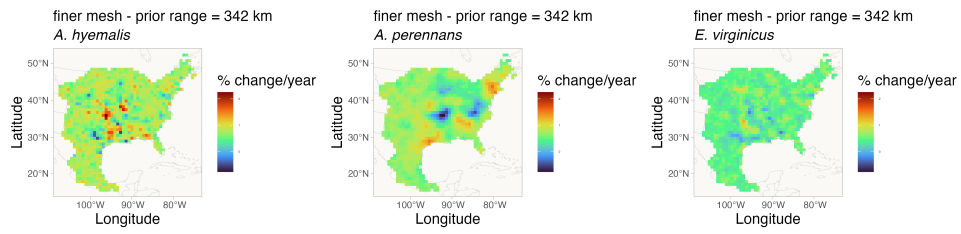
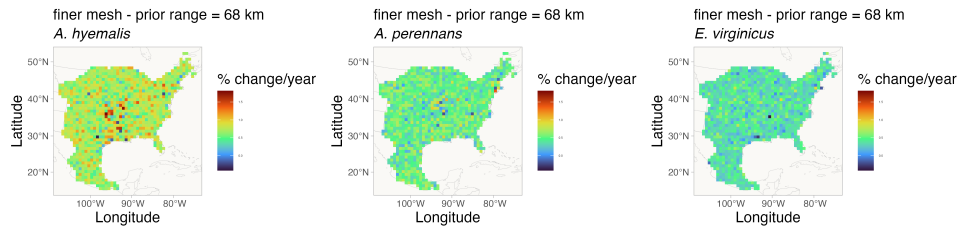


Figure A17: **Spatially-varying trends in endophyte prevalence evaluated for the endophyte prevalence model with different range priors on spatially structured random effects, and for the "standard" mesh.** Data used in model fitting is the same across all panels and as in the main text. Shading indicates the magnitude and direction of predicted trends for each of three host species for each of three prior ranges (rows A-C). Note that each plot has an individual scale bar.

A



B



C

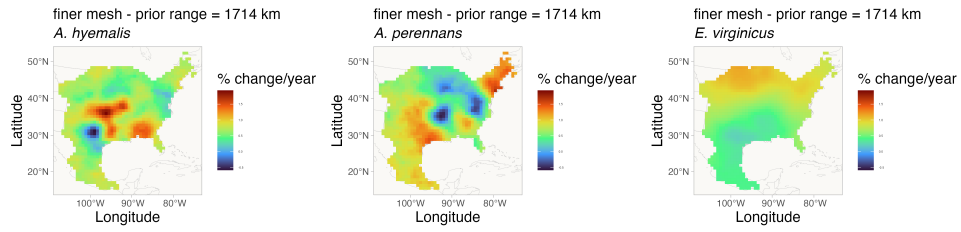


Figure A18: **Spatially-varying trends in endophyte prevalence evaluated for the endophyte prevalence model with different range priors on spatially structured random effects, and for the "finer" mesh.** Data used in model fitting is the same across all panels and as in the main text. Shading indicates the magnitude and direction of predicted trends for each of three host species for each of three prior ranges (rows A-C). Note that each plot has an individual scale bar.

1093

## *Spatially-biased Sample Size Simulation Analysis*

1094 To examine how data that is unevenly distributed across host distributions may influence interpreta-  
1095 tion of spatially-varying coefficients, we performed a simulation analysis. Our focal species, *Agrostis*  
1096 *hyemalis*, *Agrostis perennans*, and *Elymus virginicus*, are widely distributed grasses across the east-  
1097 ern United States that host *Epichloë* fungal endophytes. For logistical reasons, our sampling visits  
1098 to herbaria focused on herbaria in the central southern U.S., which resulted in unevenly distributed  
1099 data across each host species' range. This is particularly noteable for *Agrostis perennans* which has  
1100 the most northern distribution and relatively fewer total collected specimens compared to the other  
1101 focal species. Thus, a significant portion in the northeast of this species' range is relatively sparsely  
1102 sampled. Our analysis presented in the main text identified this region as having strong increase in  
1103 endophyte prevalence. Future visits to herbaria with regional focuses in the Northeastern US would  
1104 certainly garner new specimens that could provide valuable insights into shifting host and symbiont  
1105 distributions.

1106 *Simulation of spatially-biased symbiont occurrence data*

1107 We simulated datasets with varying levels of missing-ness to examine how this missing-ness influ-  
1108 enced the estimation of spatially-varying trend estimates. We first generated 300 data points for  
1109 each of three hypothetical species at random positions across an area approximating the scale of  
1110 our focal data. Each data point was randomly assigned a year of collection across 200 years. We  
1111 then simulated data from a Bernoulli process with trends alternating across nine regions (Fig. A19)  
1112 in a 3X3 grid pattern. This grid pattern was intended to create a complex spatial layout of trends,  
1113 where trends were either an increase of 1% per year or a decrease of 1% per year.

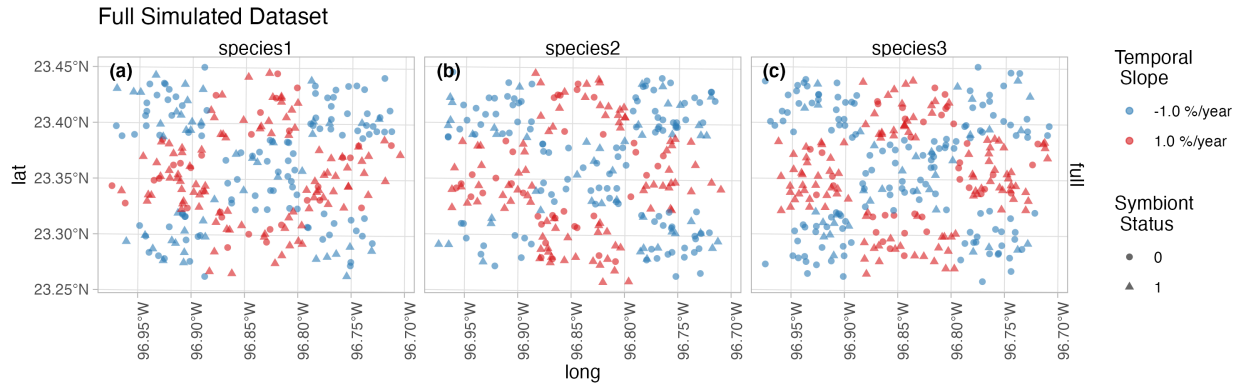
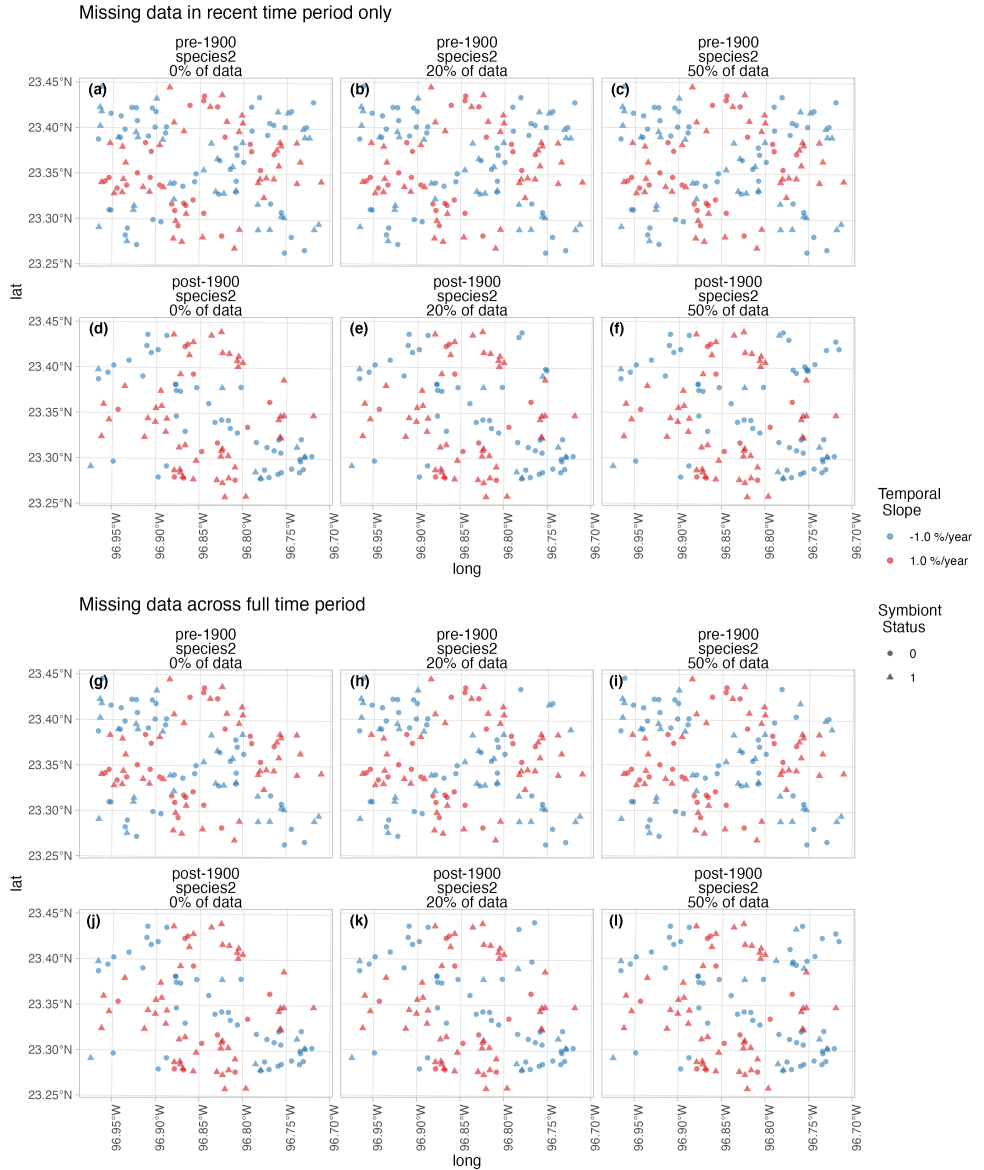


Figure A19: **Full simulated dataset of symbiotic association with spatially-varying temporal trends.** Color indicates the slope parameter used to simulate trends in endophyte status across nine "regions" for three species. Data are assigned collection years across a period of 200 years. Shape indicates the presence (1) or absence (0) of a symbiont.

1114 From this full data, we generated six additional datasets with missing-ness in the northeast  
 1115 region of the simulated data for hypothetical species 2. The data remained the same for Species 1  
 1116 and for species 3 across all datasets. For these six datasets, we removed data points at random in  
 1117 six ways: 0% of datapoints in northeast region, 0% of recent datapoints, only 20% of datapoints,  
 1118 only 20% of recent datapoints, only 50% of datapoints, and only 50% of recent datapoints (Fig.  
 1119 A20). We define the datapoints as part of the recent time period if they occur later than the median  
 1120 year. The result is 6 scenarios exploring degrees of spatial and temporal bias.



**Figure A20: Six simulated datasets representing scenarios of spatially-baised missingness for Species 2.** Missingness was imposed in the northeast region for six scenarios: 0% of recent datapoints available (a,d); only 20% of recent datapoints (b,e); only 50% of recent datapoints (c,f); 0% of datapoints across the full time period available (g,j); only 20% of datapoints across the full time period (h,k); and only 50% of datapoints across the full time period(i,l). Missingness was imposed only for hypothetical Species 2; Species 1 and 3 remain as in Figure A19. Color indicates the slope parameter used to simulate trends in endophyte status across 9 regions in a 3x3 grid. Shape indicates the presence (1) or absence (0) of a symbiont.

1121 *Statistical analysis*

1122 We analyzed each dataset with a model given by Eqn. A1 similar in construction to that used in  
1123 our central analysis.

$$\text{logit}(\hat{P}_{h,i}) = A_h + T_h * \text{year}_i + \alpha_{h,l_i} + \tau_{h,l_i} * \text{year}_i + \delta_{l_i} \quad (\text{A1})$$

1124 Where symbiont presence/absence of the  $i^{th}$  specimen ( $P_{h,i}$ ) was modeled as a Bernoulli re-  
1125 sponse variable with expected probability of symbiont occurrence  $\hat{P}_{h,i}$  for each host species  $h$ . We  
1126 modeled  $\hat{P}_{h,i}$  as a linear function of intercept  $A_h$  and slope  $T_h$  defining the global trend in endophyte  
1127 prevalence specific to each host species as well as with spatially-varying intercepts  $\alpha_{h,l_i}$  and slopes  
1128  $\tau_{h,l_i}$  associated with location ( $l_i$ , the unique latitude-longitude combination of the  $i$ th observation).  
1129 Similar to the SVC model of our central analysis (Eqn. 1), we estimated a shared variance term  
1130 with the spatially-dependent random effect  $\delta_{l_i}$ , intended to account for residual spatial variation.  
1131 However in this analysis we omit i.i.d.-random effects terms associated with collector and scorer  
1132 identity ( $\chi_{c_i}$  and  $\omega_{s_i}$  in Eqn. 1) for the sake of simplicity.

1133 *Influence of spatially-biased sampling on model interpretation*

1134 Our analysis of the full simulated data shows that our model is suitably flexible to capture complex  
1135 spatial patterns in temporal trends (Fig. A21 a-c). Beyond this, the model also qualitatively  
1136 captures the spatial patterns in temporal trends even with large amounts of data missingness (i.e  
1137 missing up to 80% of the datapoints (Fig. A21 p-r)).

1138 While this analysis is not an exhaustive examination of the influence of sampling bias on our  
1139 results for several reasons (including not examining how different strengths in temporal trends,  
1140 different spatial arrangements of missing-ness influence model estimates, or different sample sizes  
1141 influence results), it demonstrates that the spatially-varying modelling framework implemented in  
1142 INLA we employ can suitably recover regional trends even with significant spatially-bias within  
1143 data collection, and further the analysis is likely robust to temporally-structured bias (missing data

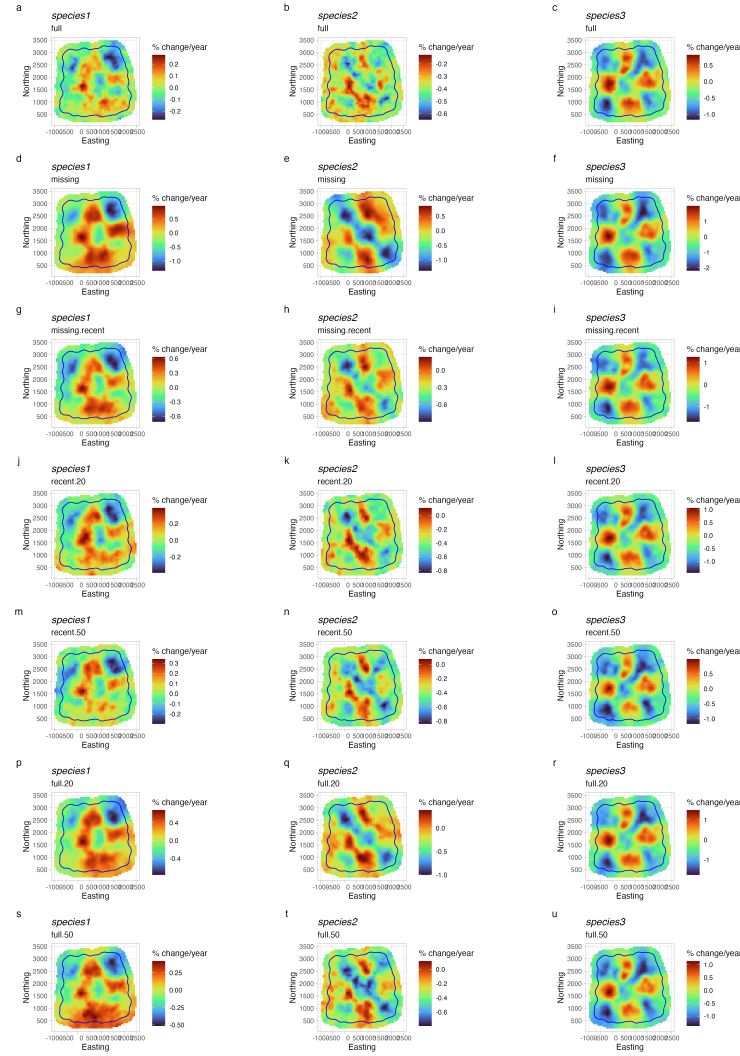


**Figure A21: Mean predicted spatially-varying trend in symbiont prevalence across datasets with different levels of missingness.** Color indicates the estimated mean temporal trend within each pixel across the simulated data. Panels show estimates for models fit to different levels of missing data for species 2 in the northeast region ((a-c) the full dataset, (d-f) missing all datapoints across entire temporal period, (g-i) missing all datapoints only during the recent period, (j-l) missing 80% of the datapoints only during the recent period, (m-o) missing 50% of the datapoints only during the recent period, (p-r) missing 80% of the datapoints across the entire temporal period, (s-u) missing 50% of the datapoints across the entire temporal period). The mesh boundary that bounds the "full" simulated dataset is plotted in each panel.

1144 within recent collection period). Future work could more fully explore the scenarios that cause  
1145 this ability to break down. We expect this simulation reflects what may be a common scenario for  
1146 research investigating global change using natural history specimens. Collection effort by trained  
1147 taxonomists and professional collectors peaked in the past, and collections contain relatively fewer  
1148 modern specimens in many regions. Additionally, most global change research necessarily involves  
1149 accessing many specimens across collections. Research efforts such as ours will be unable to access  
1150 every specimen from all possible collections. Ongoing digitization efforts will make it possible to  
1151 more clearly assess how much data is missing from a particular study compared to the actual  
1152 holdings of natural history collections, but ultimately, the decision of what data and collections to  
1153 include is a question of sample size and study design.